Low Energy antikaon-nucleon/nuclei interaction studies by AMADEUS

HYP2018

The 13th International Conference on Hypernuclear and Strange Particle Physics
June 24-29, 2018
Portsmouth

Kristian Piscicchia*
Laboratori Nazionali di Frascati (INFN)
Centro Fermi

kristian.piscicchia@lnf.infn.it

Low-energy QCD in the u-d-s sector

Investigation of **in-medium modification of the $\bar{K}N$ interaction** fundamental for the low-energy QCD in the non perturbative regime.

Chiral perturbation theory (ChPT): effective field theory where mesons and baryons represent the effective degrees of freedom instead of the fundamental quark and gluon fields.

$$\mathcal{L}_{eff} = \mathcal{L}_{mesons}(\Phi) + \mathcal{L}_B(\Phi, \Psi_B)$$

- chiral symmetry is **spontaneously broken** → existence of massless and spinless Nambu-Goldstone bosons which are identified with the pions (SU(2)). Explicitly broken by quark masses.
- **very successful** in describing the πN, ππ and NN interactions in the low-energy regime.

Problematic extension of the theory to the s sector, not directly applicable to the $\bar{K}N$ channel. See talk by A. Ramos

Low-energy QCD in the u-d-s sector

ChPT not applicable to the KN channel due to the emerging of the Λ(1405) and the Σ(1385) resonances just below the KN mass threshold (~1432 MeV)

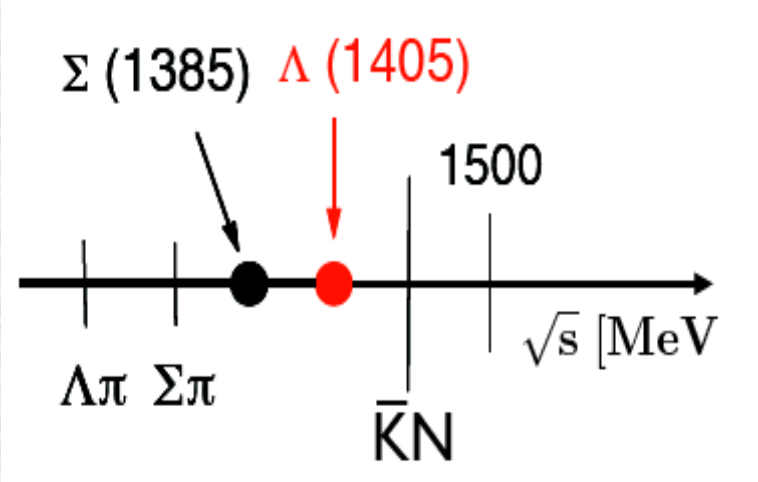

- Λ(1405) I=0 $J^P = ½^-$
  M = $(1405.1^{+1.3}_{-1.0})$ MeV Γ = (50.5 ± 2.0)

  decay modes: Σπ (I=0) 100%

- Σ(1385) I=1 $JP = 3/2^+$
  decay modes: Λ π (I=1) (87.0 ± 1.5) %
  Σ π (I=1) (11.7 ± 1.5) %

Possible solutions:

- **Non-perturbative Coupled Channels approach: Chiral Unitary SU(3) Dynamics**
- **Phenomenological K̄N and NN potentials**

Low-energy QCD in the u-d-s sector

The parameters of the models are constrained by the existing scattering data → above the threshold

Phen. [Y. Ikeda and T. Sato, Phys. Rev. C76, 035203 (2007)]
Chiral [S. Ohnishi, Y. Ikeda, T. Hyodo, W. Weise, Phys.Rev. C93 (2016) no.2, 025207]

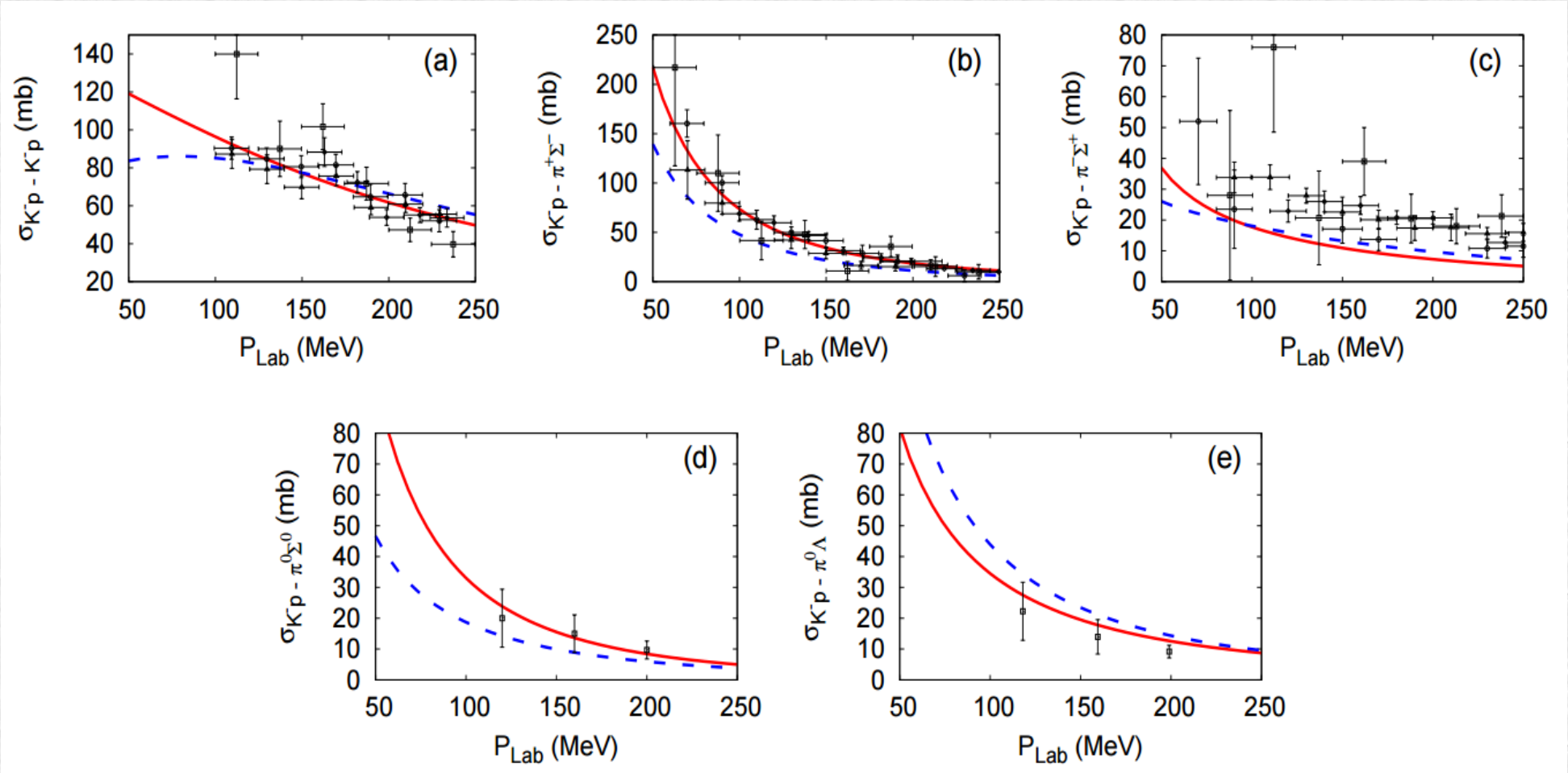

Low-energy QCD in the u-d-s sector

...but... large differences in the subthreshold extrapolations!
Significantly weaker attraction in chiral SU(3) models than in phenomenological potential models. See talk by J. Mares

Re Im

Phen. [Y. Akaishi, T. Yamazaki, Phys. Rev. C65, 044005 (2002)]
Chiral [Y. Ikeda, T. Hyodo, W. Weise, Phys. Lett. B706, 63 (2011)]

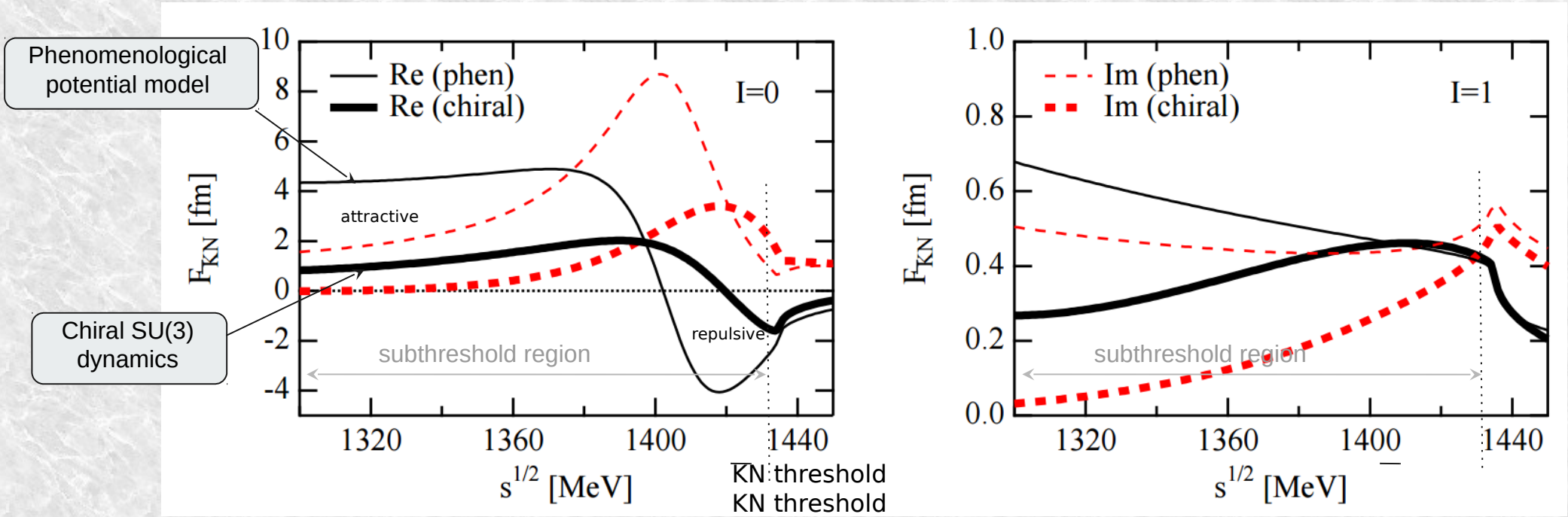

The Λ(1405) case

- **Chiral unitary models: Λ(1405) is an I = 0 quasibound state emerging from the coupling between the $\bar{K}N$ and the Σπ channels. Two poles in the neighborhood of the Λ(1405):**

***two poles*: about 1420 ; about = 1380 MeV (Phys. Lett. B 500 (2001), Phys. Rev. C 66 (2002), (Nucl. Phys. A 725 (2003) 181) .. many others .. (Nucl. Phys. A881, 98 (2012)) .. others**

mainly coupled to $\bar{K}N$ **mainly coupled to Σπ → line-shape depends on the production mechanism**

- **Akaishi-Esmaili-Yamazaki phenomenological potential**

Phys. Lett. B 686 (2010) 23-28
Confirmation of single pole ansatz?

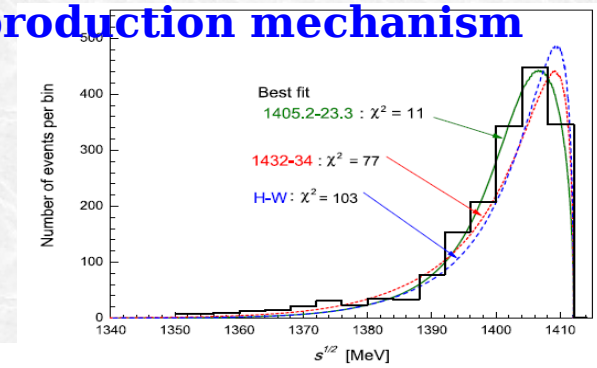

erences in $M_{\Sigma\pi}$ spectra among the Hyodo–Weise prediction and predictions.

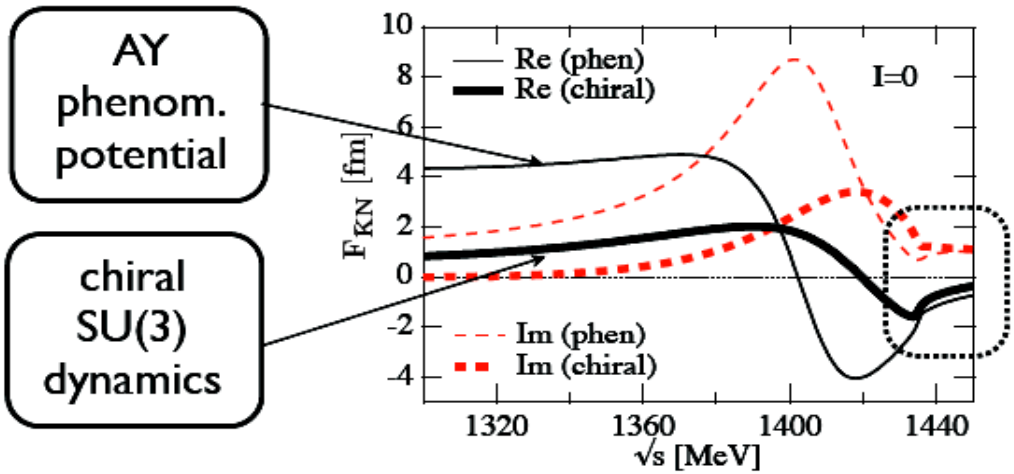

large differences in **subthreshold** extrapolations

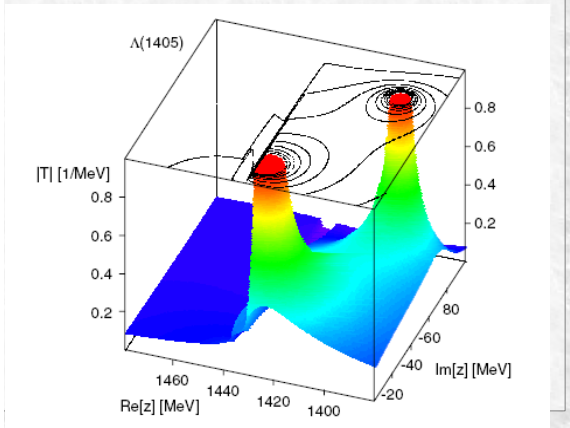

- **Chiral dynamics** predicts significantly **weaker attraction** than AY (local, energy independent) potential in **far-subthreshold** region

The Λ(1405) case

BUBBLE CHAMBER search of the Λ(1405):

- O. Braun et al. Nucl. Phys. B129 (1977) 1

K- induced reactions on d $\rightarrow$ $\Sigma^- \pi^+$ n the resonance is found & 1420 MeV

- D. W. Thomas et al., Nucl. Phys. B56 (1973) 15

pion induced reaction π^- p $\rightarrow$ $K^+ \pi$ Σ the resonance is found & 1405MeV

- R. J. Hemingway, Nucl. Phys. B253 (1985) 742

$K^- p \rightarrow \pi^- \Sigma^+(1660) \rightarrow \pi^- (\pi^+ \Lambda(1405)) \rightarrow \pi^- \pi^+ (\pi\Sigma)$ & 4.2 GeV

analysed by Dalitz and Deloff M = 1406.5 ± 4.0 MeV, Γ = 50 ± 2MeV

- HADES coll. Phys. Rev. C 87, 025201 (2013)

$p\,p \rightarrow p\, K^+ \pi\Sigma$ the resonance is found & 1390 MeV

The Λ(1405) case

THE "LINE-SHAPE" OF THE Λ(1405) DEPENDS ON THE OBSERVED CHANNEL !!

$$\frac{d\sigma(\Sigma^-\pi^+)}{dM} \propto \frac{1}{3}\left|T^0\right|^2 + \frac{1}{2}\left|T^1\right|^2 + \frac{2}{\sqrt{6}}Re(T^0T^{1*})$$

$$\frac{d\sigma(\Sigma^+\pi^-)}{dM} \propto \frac{1}{3}\left|T^0\right|^2 + \frac{1}{2}\left|T^1\right|^2 - \frac{2}{\sqrt{6}}Re(T^0T^{1*})$$

$$\frac{d\sigma(\Sigma^0\pi^0)}{dM} \propto \frac{1}{3}\left|T^0\right|^2$$

The Λ(1405) case

THE "LINE-SHAPE" OF THE Λ(1405) DEPENDS ON THE OBSERVED CHANNEL !!

$$\frac{d\sigma(\Sigma^-\pi^+)}{dM} \propto \frac{1}{3}\left|T^0\right|^2 + \frac{1}{2}\left|T^1\right|^2 + \frac{2}{\sqrt{6}}Re(T^0T^{1*})$$

$$\frac{d\sigma(\Sigma^+\pi^-)}{dM} \propto \frac{1}{3}\left|T^0\right|^2 + \frac{1}{2}\left|T^1\right|^2 - \frac{2}{\sqrt{6}}Re(T^0T^{1*})$$

$$\frac{d\sigma(\Sigma^0\pi^0)}{dM} \propto \frac{1}{3}\left|T^0\right|^2$$

IS DIFFERENT IN $\Sigma^+\pi^-$ VS $\Sigma^-\pi^+$

DUE TO ISOSPIN INTERFERENCE

The Λ(1405) case

THE "LINE-SHAPE" OF THE Λ(1405) DEPENDS ON THE OBSERVED CHANNEL !!

$$\frac{d\sigma(\Sigma^-\pi^+)}{dM} \propto \frac{1}{3}\left|T^0\right|^2 + \frac{1}{2}\left|T^1\right|^2 + \frac{2}{\sqrt{6}}Re(T^0T^{1*})$$

$$\frac{d\sigma(\Sigma^+\pi^-)}{dM} \propto \frac{1}{3}\left|T^0\right|^2 + \frac{1}{2}\left|T^1\right|^2 - \frac{2}{\sqrt{6}}Re(T^0T^{1*})$$

$$\frac{d\sigma(\Sigma^0\pi^0)}{dM} \propto \frac{1}{3}\left|T^0\right|^2$$

IS DIFFERENT IN $\Sigma^+\pi^-$ VS $\Sigma^-\pi^+$

DUE TO ISOSPIN INTERFERENCE

THE CLEANEST SIGNATURE OF THE Λ(1405) IS GIVEN BY THE NEUTRAL CHANNEL:

- is free from isospin interference
- is purely I = 0, no Σ(1385) contamination.

Λ(1405) .. the golden channel

Crystall Ball: K-p → $\Sigma^0\pi^0\pi^0$ for kaon momentum in the range (514-750 MeV/c). S. Prakhov et al. Phys Rev. C70 (2004) 03465

(**interpreted by Magas et al. PRL 95, 052301 (2005)**)

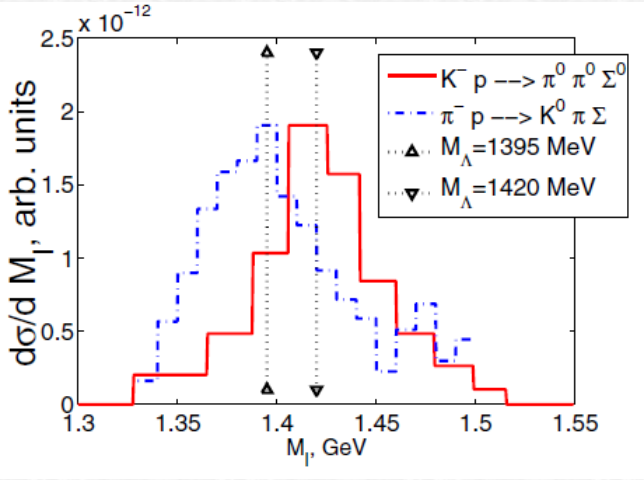

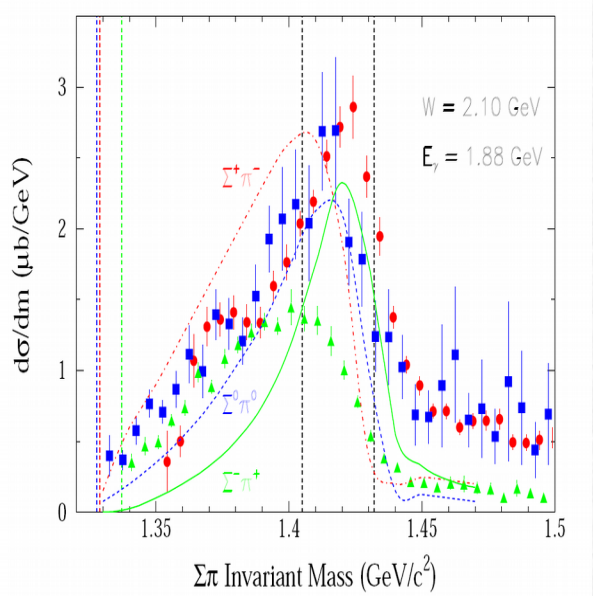

CLAS: γ p → K+ $\Sigma\pi$

AIP Conf.Proc. 1441 (2012) 296-298

COSY julich: pp → pK+ $\Sigma^0\pi^0$

(I. Zychor et al., Phys. Lett. B 660 (2008) 167)

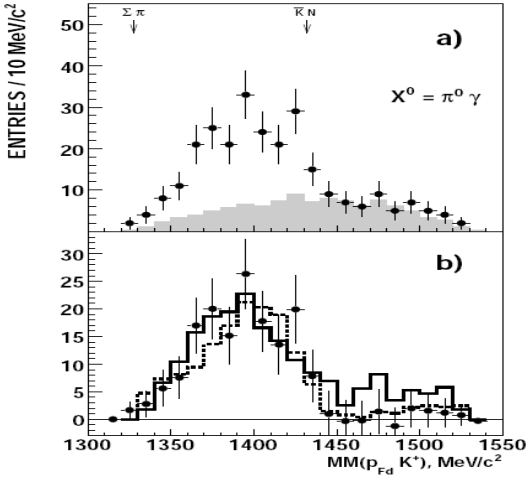

Fig. 4. a) Missing–mass $MM(p_{Fd}K^+)$ distribution for the $pp \to pK^+p\pi^-X^0$ reaction for events with $M(p_{Sd}\pi^-) \approx m(\Lambda)$ and $MM(pK^+p\pi^-) > 190\,\mathrm{MeV/c^2}$. Exper-

Λ(1405) .. the golden channel

Crystall Ball: K-p → $\Sigma^0\pi^0\pi^0$ for kaon momentum in the range (514-750 MeV/c). S. Prakhov et al. Phys Rev. C70 (2004) 03465 (Magas et al. PRL 95, 052301 (2005))

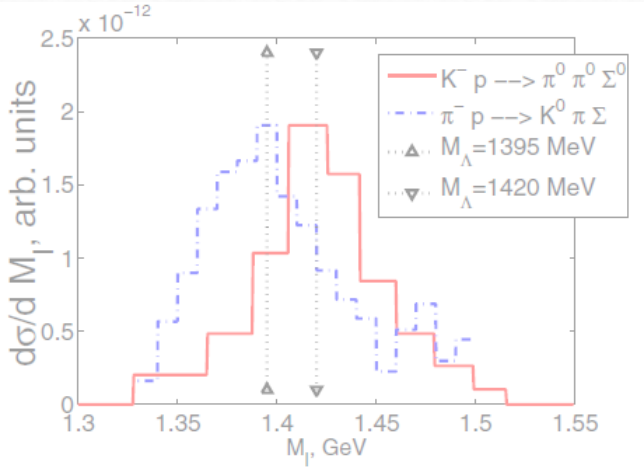

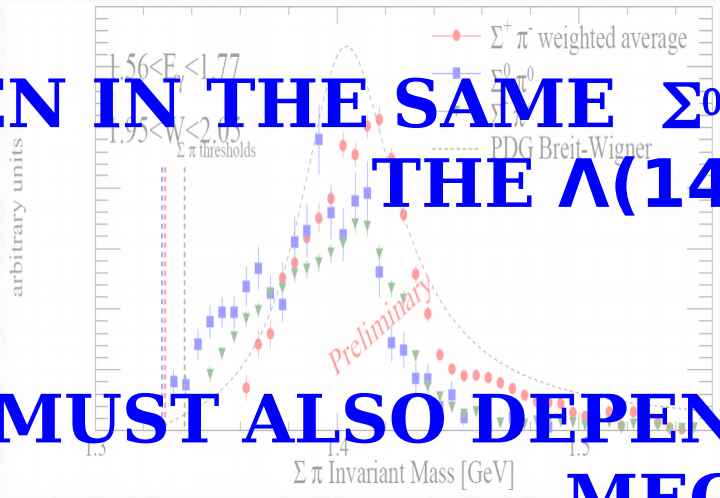

EVEN IN THE SAME $\Sigma^0\pi^0$ THE "LINE-SHAPE" OF THE Λ(1405) CHANGES

CLAS γp → pK⁺ Σπ

AIP Conf.Proc. 1441 (2012) 296-298

IT MUST ALSO DEPEND ON THE PRODUCTION MECHANISM

COSY julich: pp → pK⁺ $\Sigma^0\pi^0$

(I. Zychor et al., Phys. Lett. B 660 (2008) 167)

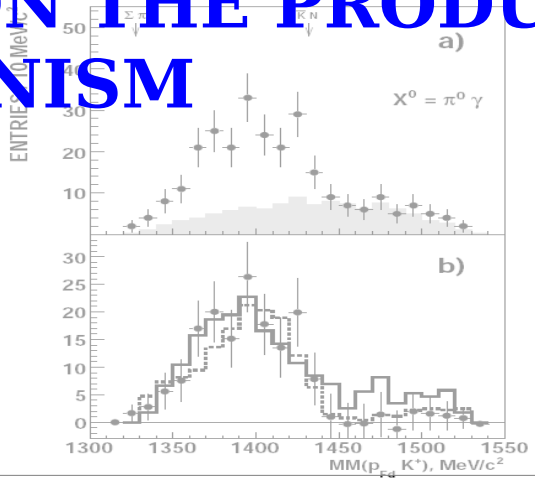

Fig. 4. a) Missing–mass $MM(p_{Fd}K^+)$ distribution for the $pp \to pK^+p\pi^-X^0$ reaction for events with $M(p_{Sd}\pi^-) \approx m(\Lambda)$ and $MM(pK^+p\pi^-) > 190\,\mathrm{MeV/c^2}$. Exper-

The Λ(1405) case

Two main biases:

- **the kinematical energy threshold 1412 MeV**

  (MK + Mp - |BEp|) the high pole energy region is closed,

- **The shape and the amplitude of the NON-RESONANT**

  Σ π production below KbarN threshold never measured.

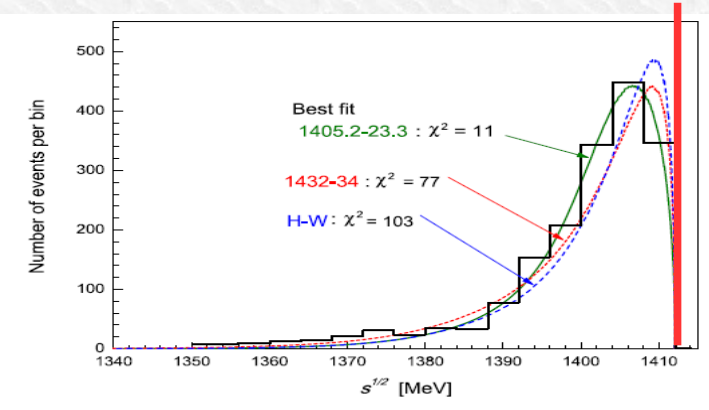

Fig. 6. Detailed differences in $M_{\Sigma\pi}$ spectra among the Hyodo–Weise prediction and the present model predictions.

An ideal experiment:

- **Λ(1405) is produced in K- p absorption → mainly coupled to the high mass pole,**
- **Λ(1405) is observed in the $\Sigma^0\pi^0$ decay channel (almost pure isospin 0),**
- **K- is absorbed in-flight on a bound proton with p_K ~ 100 MeV, Σπ invariant mass gain of ~ 10 MeV to open an energy window to the high mass pole.**
- **Knowledge of the Σπ NON-RESONANT production amplitude.**

How deep can an antikaon be bound in a nucleus?

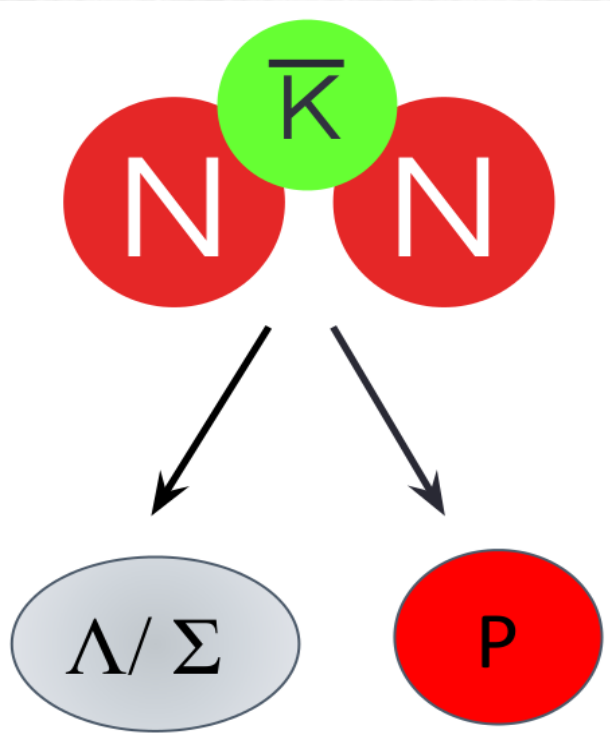

Possible Bound States:

$(K^- pp) \rightarrow \Lambda\, p$
$\rightarrow \Sigma^0\, p$

$(K^- ppn) \rightarrow \Lambda\, d$
$\rightarrow \Sigma^0\, d$

predicted if strong $\bar{K}N$ interaction in the I=0 channel.

[Wycech (1986) - Akaishi & Yamazaki (2002)]

K^-pp bound state

	BE (MeV)	Γ (MeV)	Reference
Dote, Hyodo, Weise	17-23	40-70	Phys.Rev.C79 (2009) 014003
Akaishi, Yamazaki	48	61	Phys.Rev.C65 (2002) 044005
Barnea, Gal, Liverts	16	41	Phys.Lett.B712 (2012) 132-137
Ikeda, Sato	60-95	45-80	Phys.Rev.C76 (2007) 035203
Ikeda, Kamano, Sato	9-16	34-46	Prog.Theor.Phys. (2010) 124(3): 533
Shevchenko, Gal, Mares	55-70	90-110	Phys.Rev.Lett.98 (2007) 082301
Revai, Shevchenko	32	49	Phys.Rev.C90 (2014) no.3, 034004
Maeda, Akaishi, Yamazaki	51.5	61	Proc.Jpn.Acad.B 89, (2013) 418
Bicudo	14.2-53	13.8-28.3	Phys.Rev.D76 (2007) 031502
Bayar, Oset	15-30	75-80	Nucl.Phys.A914 (2013) 349
Wycech, Green	40-80	40-85	Phys.Rev.C79 (2009) 014001

Experiments reporting DBKNS		
KEK-PS E549	T. Suzuki at al. MPLA23, 2520-2523 (2008)	
FINUDA	M. Agnello et al. PRL94, 212303 (2005)	Extraction of a **signal**
DISTO	T. Yamazaki et al. PRL104 (2010)	Extraction of a **signal**
OBELIX	G. Bendiscioli et al. NPA789, 222 (2007)	Extraction of a **signal**
HADES	G. Agakishiev et al. PLB742, 242-248 (2015)	**Upper limit**
LEPS/SPring-8	A.O. Tokiyasu et al. PLB728, 616-621 (2014)	**Upper limit**
J-PARC E15	T. Hashimoto et al. PTEP, 061D01 (2015)	**Upper limit**
J-PARC E27	Y. Ichikawa et al. PTEP, 021D01 (2015)	Extraction of a **signal**

How deep can an antikaon be bound in a nucleus?

interpreted in
T. Sekihara, E. Oset, A. Ramos, Prog. Theor. Exp. Phys (2016) (12): 123D03

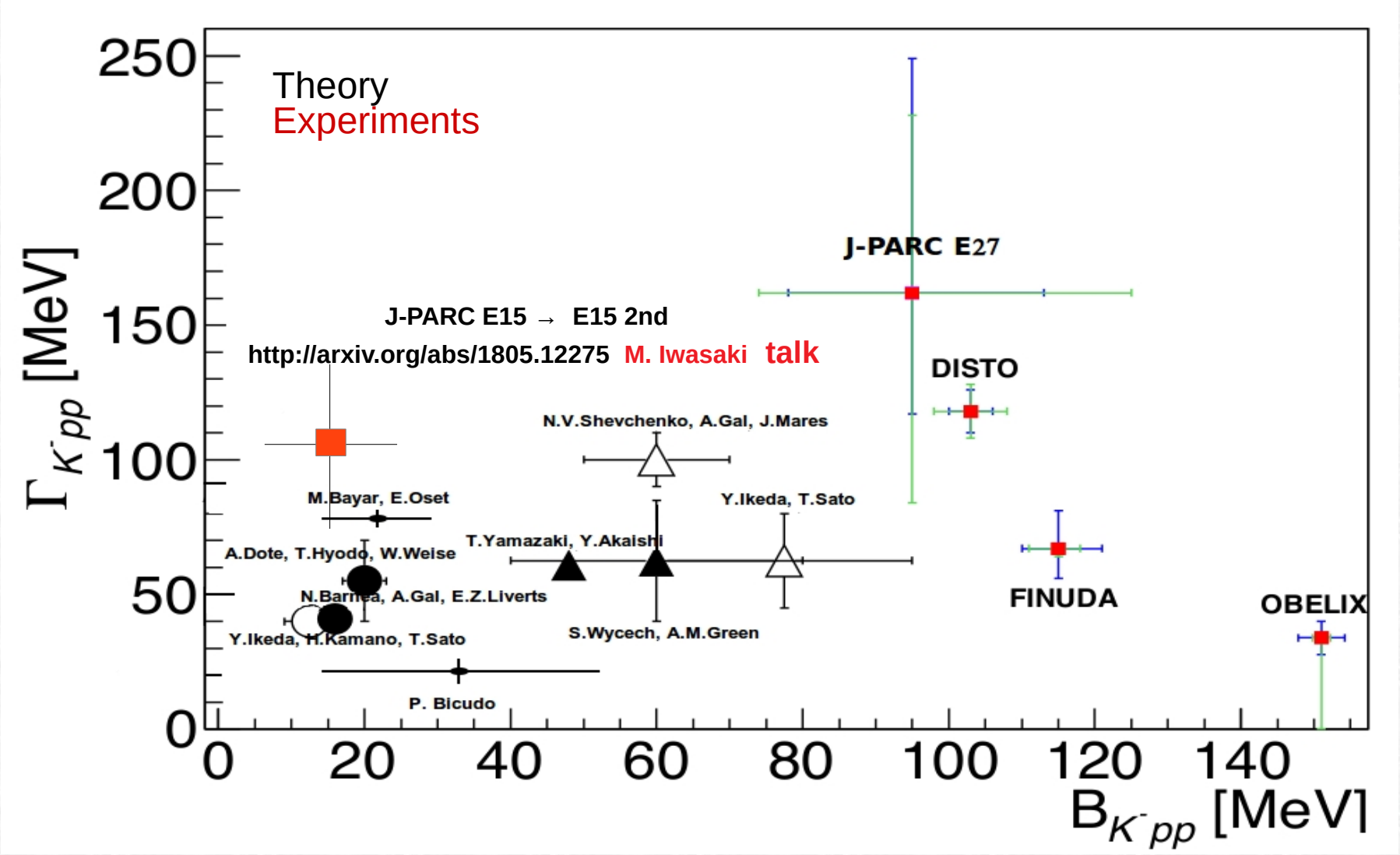

[from the talk of T. Nagae at HYP2015, Sep. 10, 2015]

Bound state search in K- induced reactions

E549 at KEK: $K^-_{stop} + {}^4He \rightarrow \Lambda + p + X'$

detected particles

[T. Suzuki et al., Mod. Phys. Lett. A23 (2008) 2520-2523.]

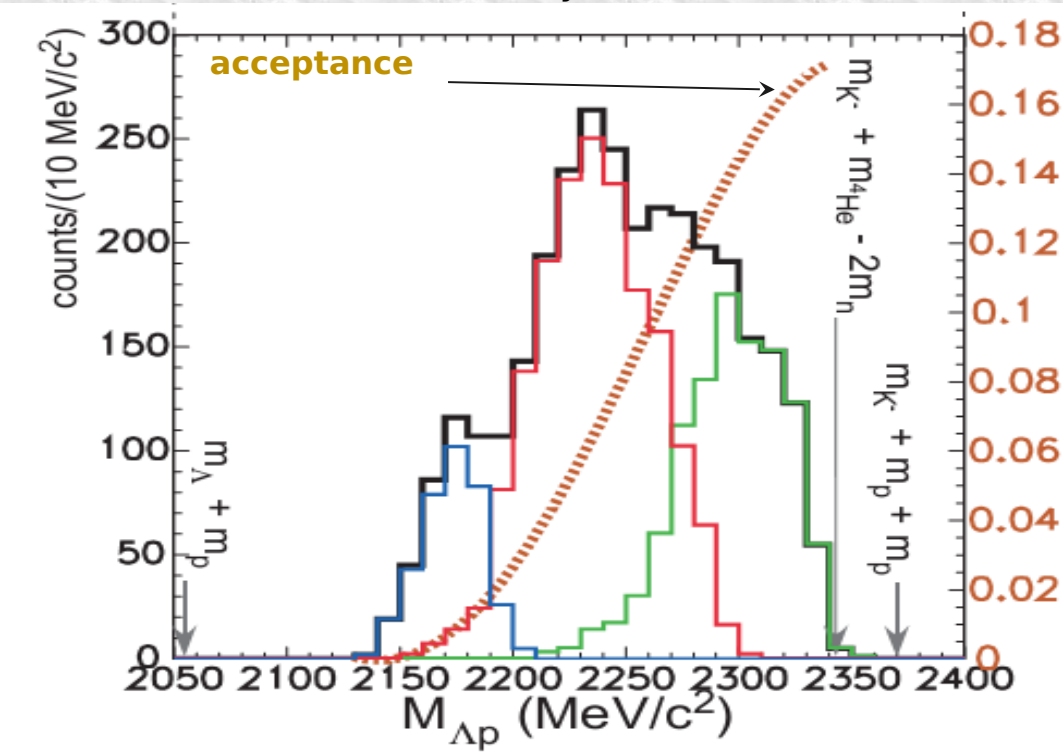

Measurement of yields and shapes of the K- multi-nucleon yields is mandatory to solve the puzzle!

They are the counterpart of the non-resonant single nucleon capture

- **1NA**: K^- single nucleon absorption
- **2NA**: K^- two nucleon absorption
- **2NA + conversion**, **multi-nucleon**, **or Bound State**?

and K- multi-nucleon cross section?

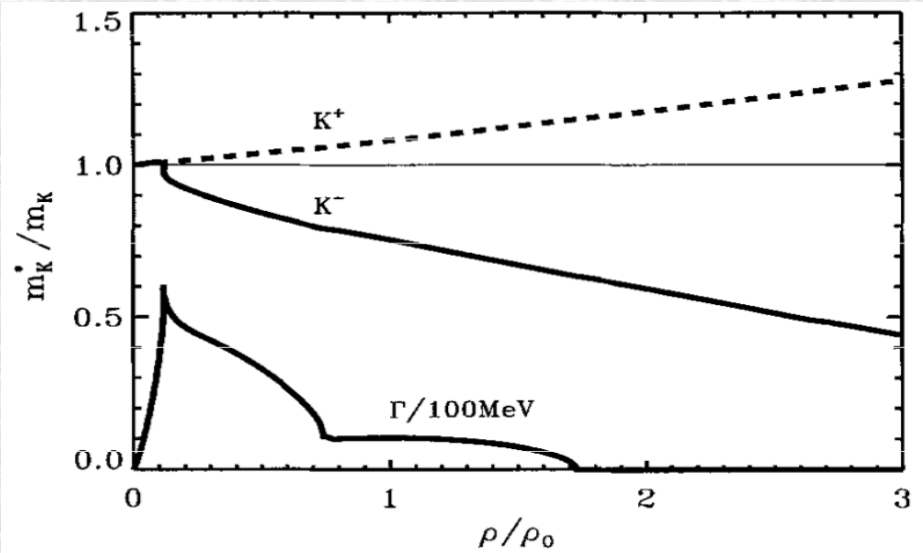

In medium $\bar{K}$ properties investigated in heavy-ion & proton nuclei collisions, K^- mass modification extrapolated from the K^- production yield

Transport models and collision calculations need the measurement of the K- multi-nucleon cross sections at low energy

...

still missing!

AMADEUS scientific case

- Nature of the $\Lambda(1405)$ & K^-N amplitude below threshold $\rightarrow$
  $Y\pi$ CORRELATION STUDIES

- **K^- multi-nucleons** absorptions cross sections
- **kaonic nuclear clusters**

$\rightarrow$ **YN CORRELATION STUDIES** (i.e. Λp, $\Sigma^0 p$, and Λt final states)

- Low-energy charged kaon **cross sections** for low momenta (100 MeV/c)

- **YN scattering** $\rightarrow$ **extremely poor experimental information from scattering data**
  (strong impact on the EoS of Neutron Stars
  Related to NS merging radiation + GW emission)

AMADEUS & DAΦNE

DAΦNE

- double ring $e^+ e^-$ collider working at C.M. energy of ϕ, producing **≈ 1000 ϕ /s**

$\phi \rightarrow K^+ K^-$ (BR = (49.2 ± 0.6)%)

- **low momentum** Kaons ≈ 127 Mev/c
- **back to back** $K^+ K^-$ topology

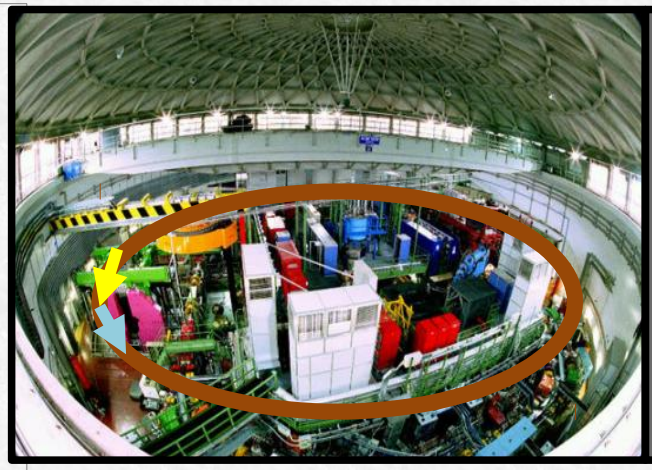

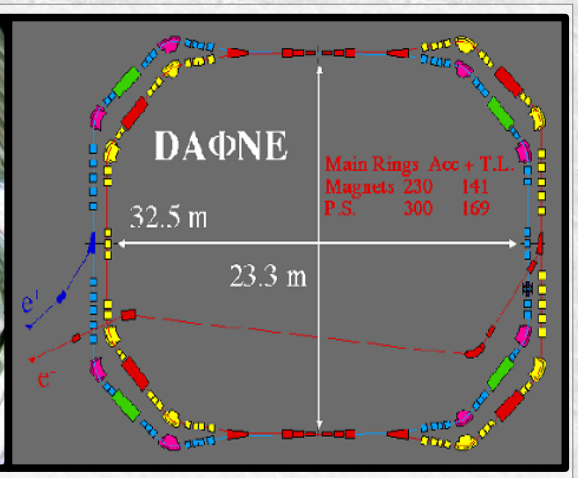

AMADEUS step 0 → KLOE 2004-2005 dataset analysis ($\mathscr{L}$ = 1.74 fb^{-1})

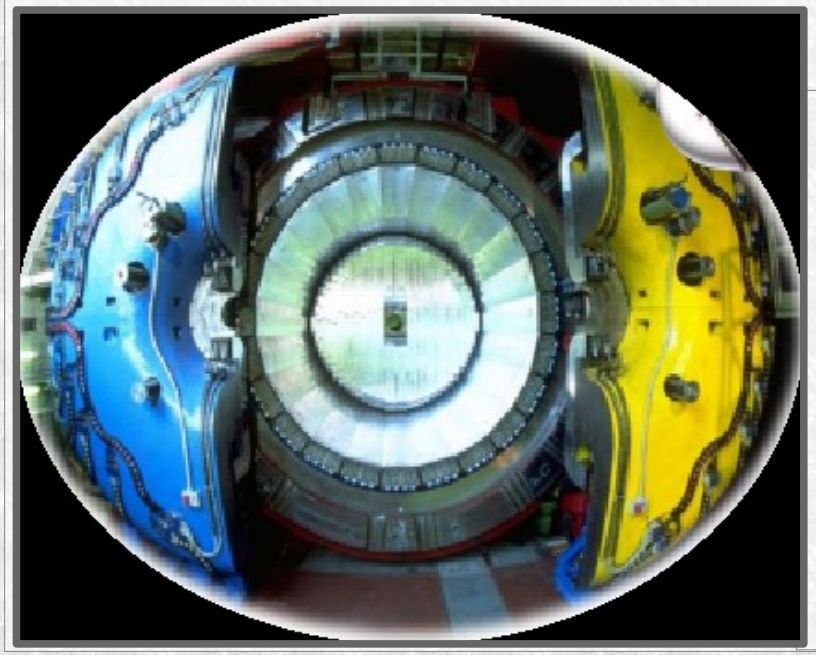

KLOE

- Cilindrical drift chamber with a **4π geometry** and electromagnetic calorimeter
- **96% acceptance**
- optimized in the energy range of all **charged particles** involved
- **good performance** in detecting **photons and neutrons** checked by kloNe group

[M. Anelli et al., Nucl Inst. Meth. A 581, 368 (2007)]

K^- absorption on light nuclei

from the materials of the KLOE detector
DC gas (90% He, 10% C_4H_{10}) & DC wall (C + H)

AT-REST (K^- absorbed from atomic orbit) or IN-FLIGHT (p_K~100MeV)

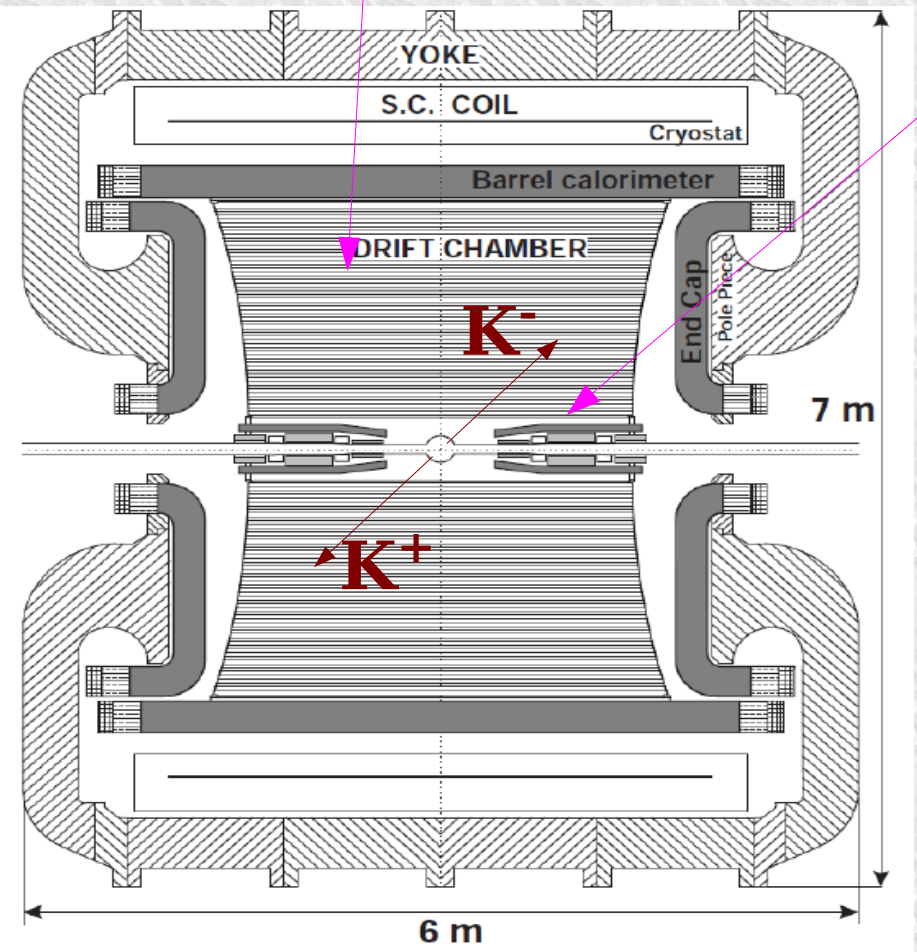

Advantage:
excellent resolution ..
$\sigma_{p\Lambda}$ = 0.49±0.01 MeV/c in DC gas
$\sigma_{m\gamma\gamma}$ = 18.3±0.6 MeV/c^2

Disadvantage:
Not dedicated target → different nuclei contamination → complex interpretation .. but → new features ..
K^- in flight absorption.

At-rest VS in-flight K^- captures

AT-REST

K^- absorbed from atomic orbit

(p_K~ 0 MeV)

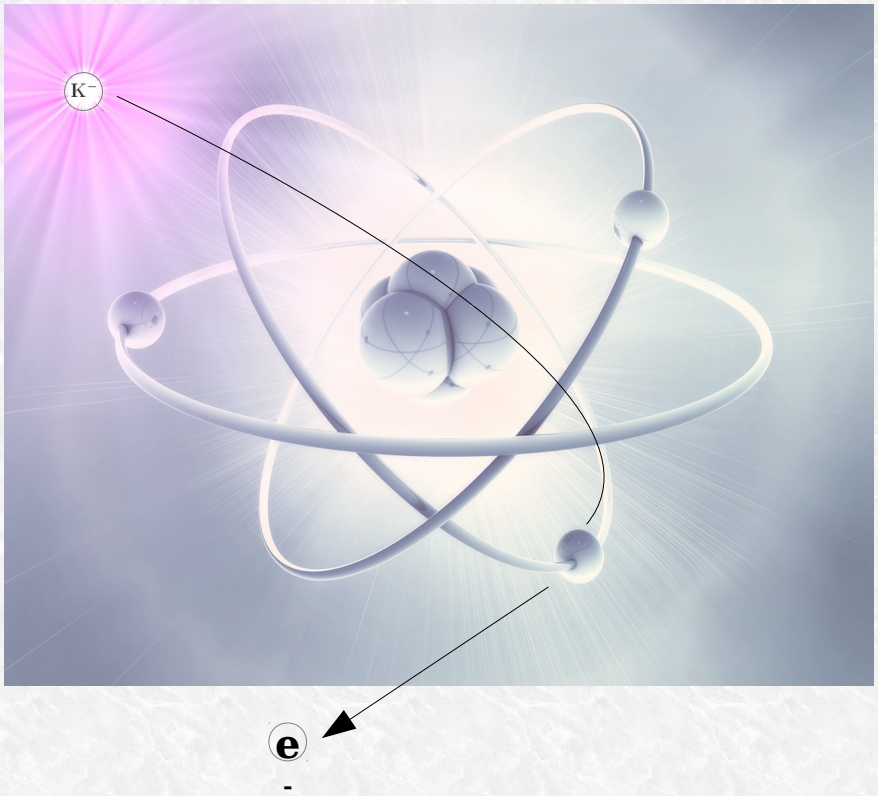

IN-FLIGHT

(p_K~100MeV)

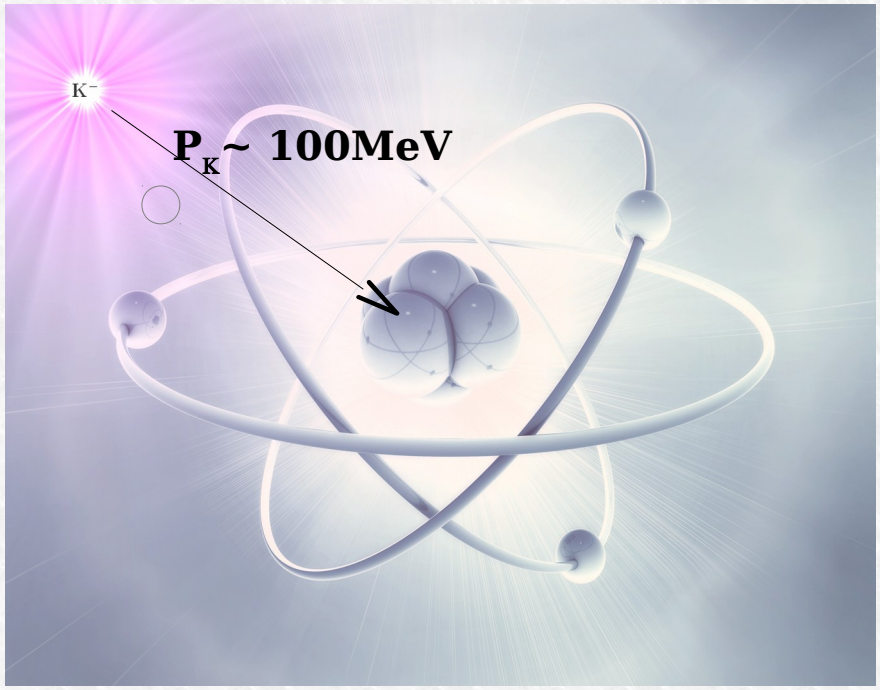

Pure graphite Carbon target

Advantages:

- **gain in statistics**
- **pure K^- Carbon absorptions**
- **pure absorptions at-rest.**

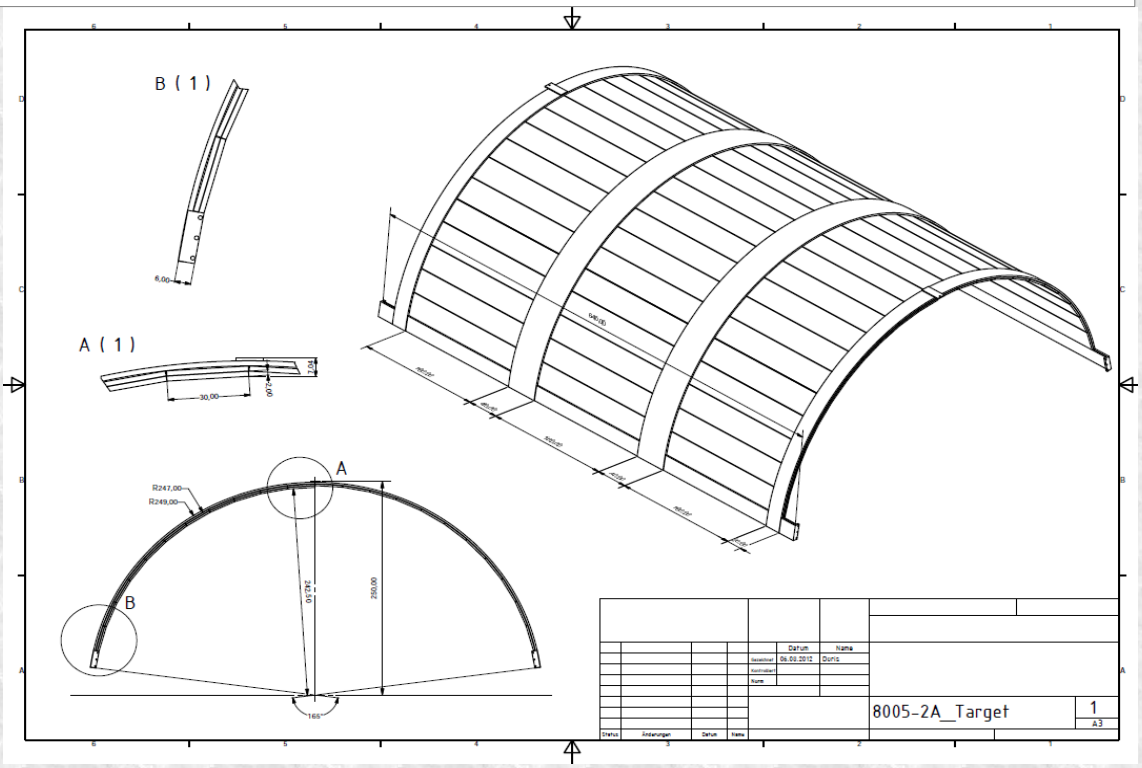

- **MC simulation: 26% of K^- stopped in ^{12}C**

- **Thickness optimized to maximize the number of stopping K^- in the targed (minimizing energy loss)**

(~90 pb^{-1}; analyzed 37 pb^{-1}, x 1.5 statistics)

K^- - N single nucleon absorption

resonant and non-resonant amplitudes

Λ(1405) case

Phys.Rev.Lett.95:052301,2005

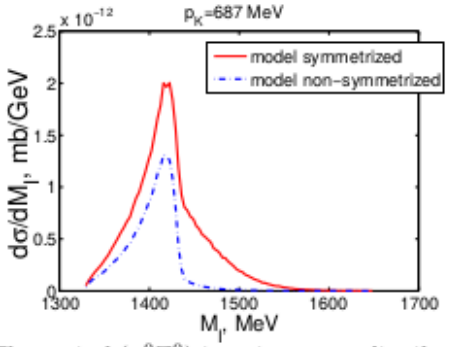

FIG. 4: Theoretical ($\pi^0\Sigma^0$) invariant mass distribution for an initial kaon lab momenta of 687 MeV. The non-symmetrized distribution also contains the factor 1/2 in the cross section.

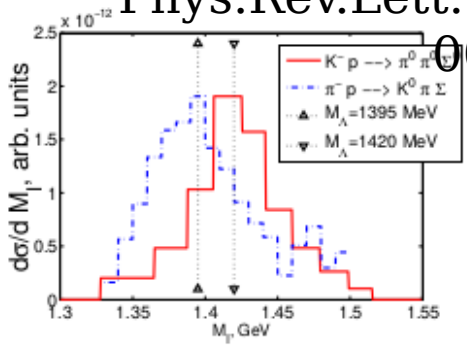

FIG. 5: Two experimental shapes of Λ(1405) resonance. See text for more details.

$p_{\pi 0}$ resolution: $\sigma_p \approx 12$ MeV/c

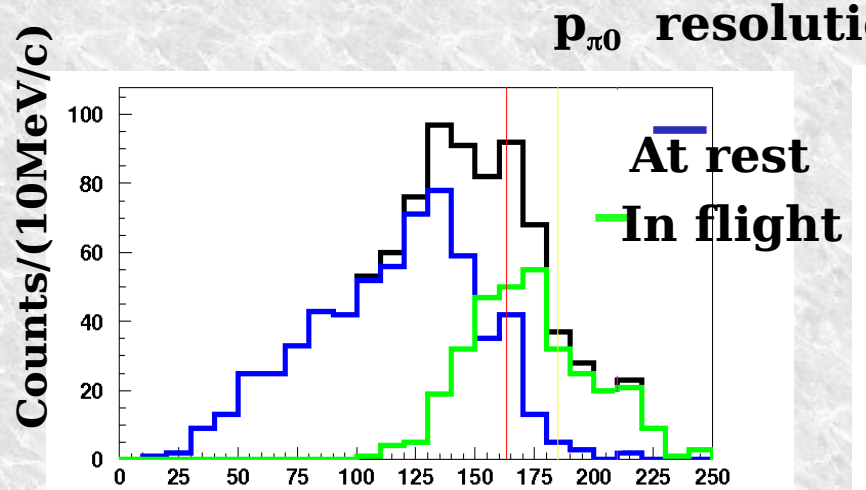

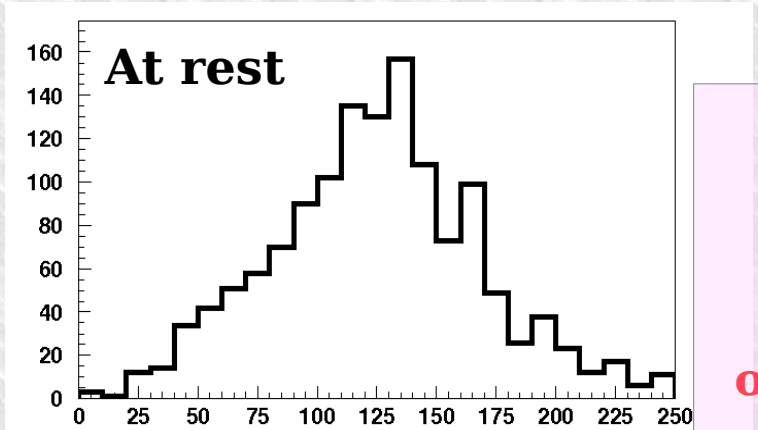

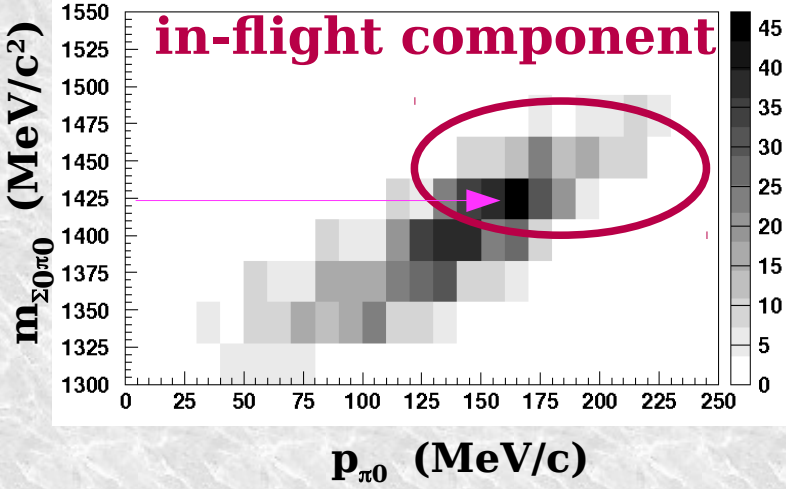

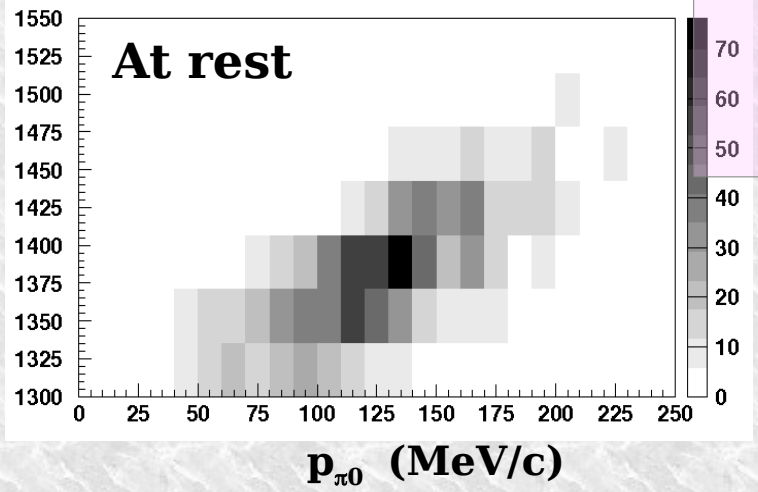

IN-FLIGHT K- 12C opens a window between 1416 MeV and K-Nth

Λ(1405) : extracting the resonant I = 0 contribution

PID optimised, data fit is ongoing

necessary the input of the $\Lambda\pi^-$ measurement

- K. Piscicchia et al., APP B48 (2017) 10, 1875
- C. Curceanu, K. Piscicchia et al., APP B46 (2015) 1, 203

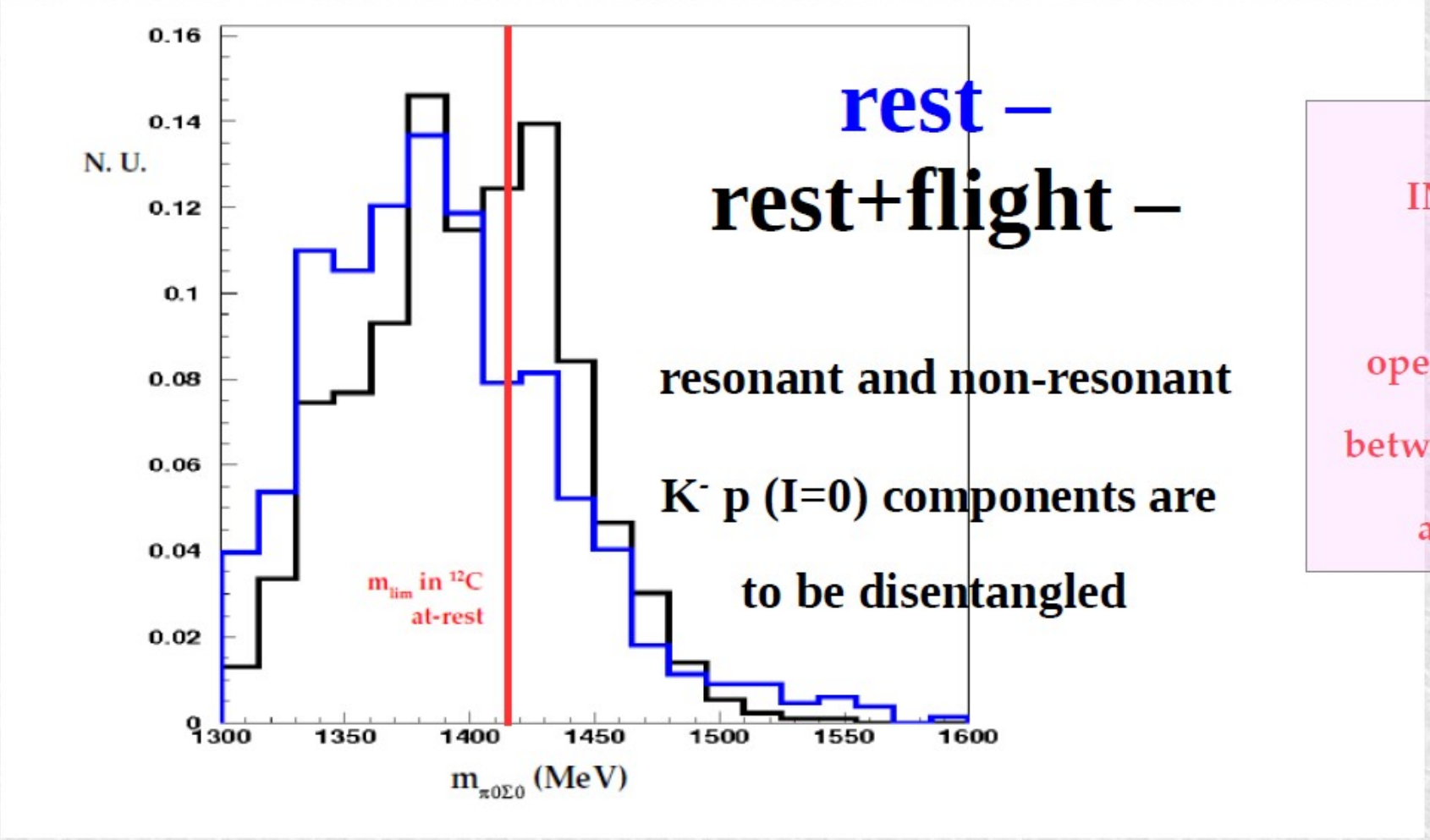

IN-FLIGHT

K- 12C

opens a window

between 1416 MeV

and K-Nth

Resonant VS non-resonant

$$K^- N \rightarrow (Y^* ?) \rightarrow Y \pi$$

how much comes from resonance ?

Non resonant transition amplitude

never measured before below threshold

can be obtained exploiting K^- N in-medium absorption,

chosen target ^{4}He

- K^- angular momentum at the capture
- absorbing nucleon wave function

} known quantities

Resonant VS non-resonant

Investigated using:

K^- "n" → $\Lambda\pi^-$ direct formation in ^{4}He

the goal is to measure **$|f^{N-R}_{\Lambda\pi}(I=1)|$**

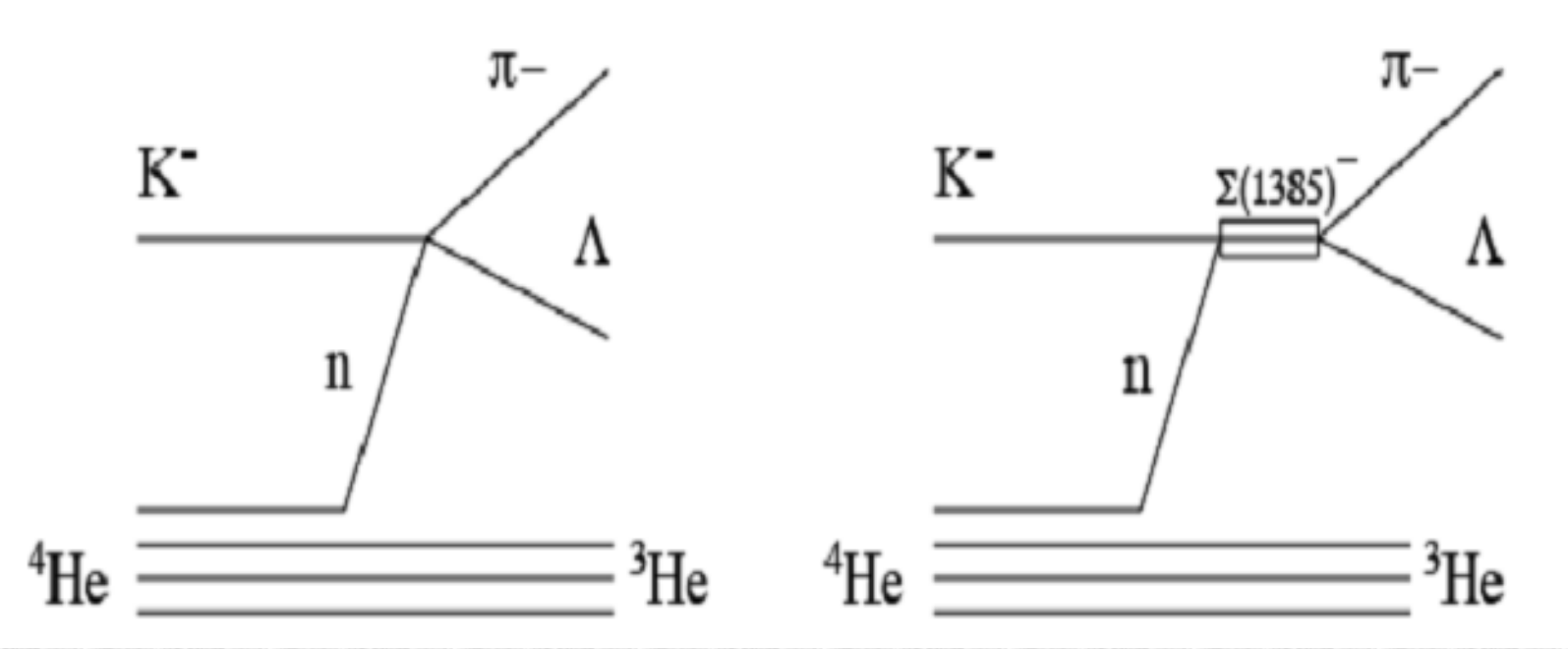

Resonant VS non-resonant

Investigated using:

K^- "n" → $\Lambda\pi^-$ to extract **$|f^{N-R}_{\Lambda\pi}(I=1)|$**

below threshold

J. Hrtankova, and J. Mares, Phys. Rev. C96, (2017) 015205
A. Cieply et al., Nucl. Phys. A954, (2016) 17

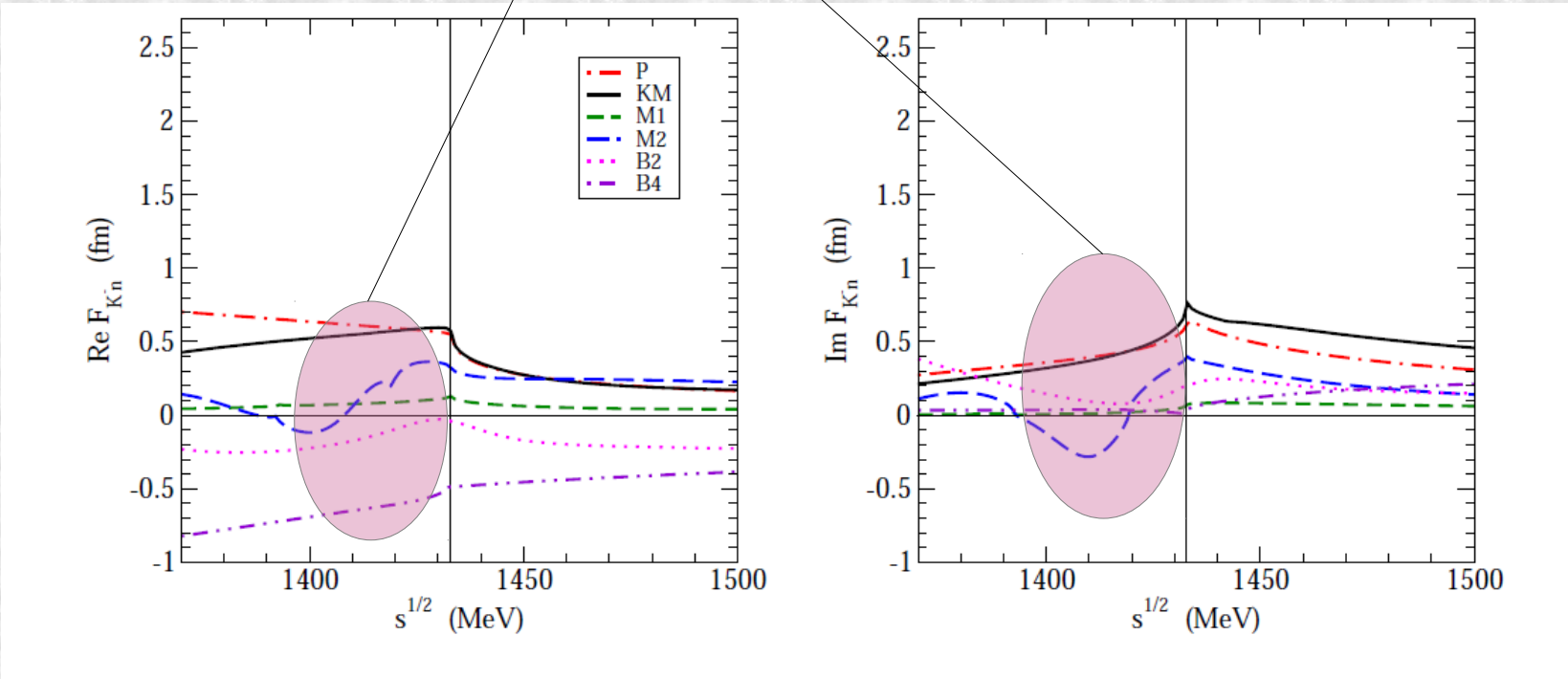

$K^- {}^4He \rightarrow \Lambda p^- {}^3He$ resonant and non-resonant processes

K. P., S. Wycech and C. Curceanu, Nucl. Phys. A954 (2016) 75-93
R. Del Grande, K. P., S. Wycech, Acta Phys. Pol. B 48 (2017) 1881

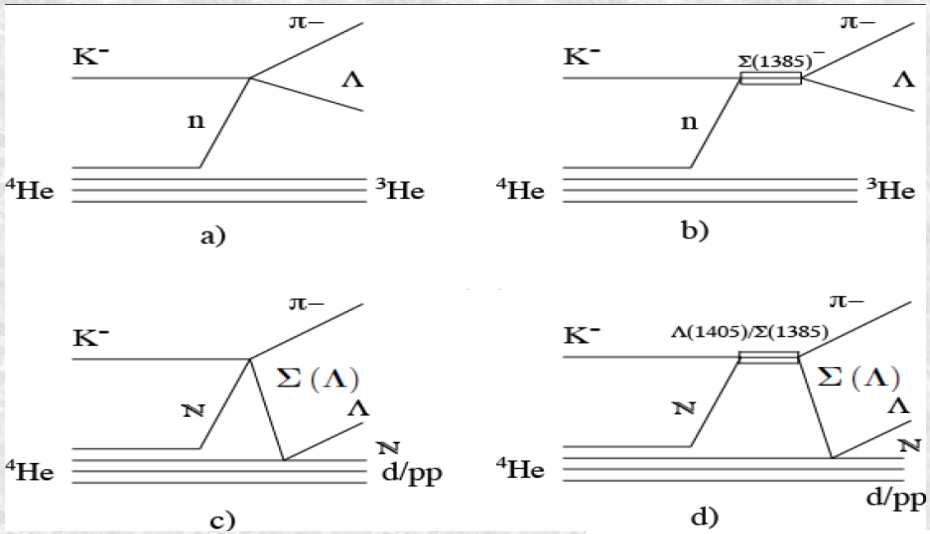

Theoretical shapes for :

total $\Lambda\pi^-$ momentum spectra for the resonant (Σ^{*-}) and non-resonant (I = 1) processes were calculated, for both S-state and P-state K^- capture at-rest and in-flight. Corrections to the amplitudes due to Λ/π final state interactions were estimated.

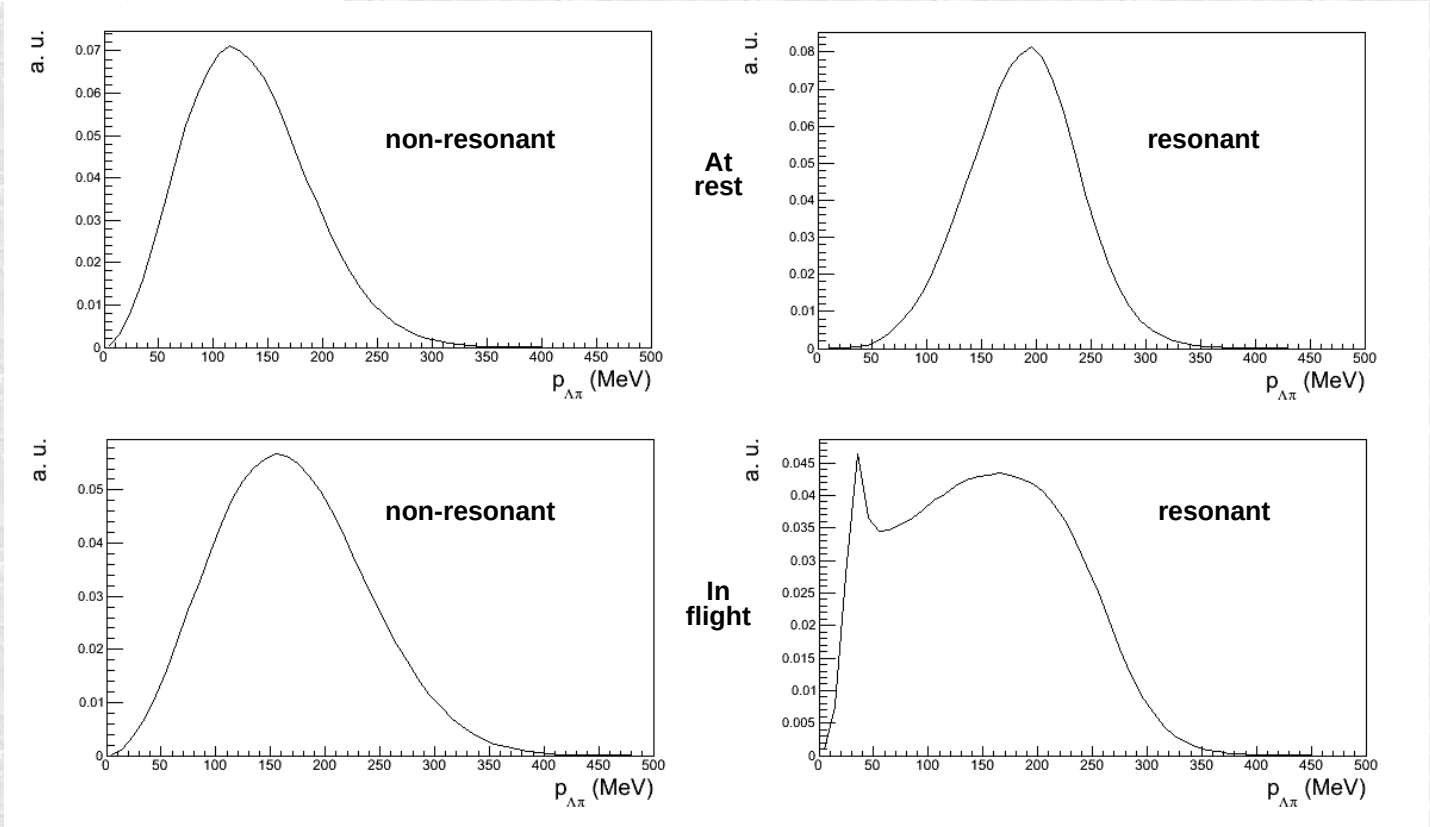

Simultaneous fit : ($p_{\Lambda\pi^-}$ - $m_{\Lambda\pi^-}$ - $\cos(\theta_{\Lambda\pi^-})$)

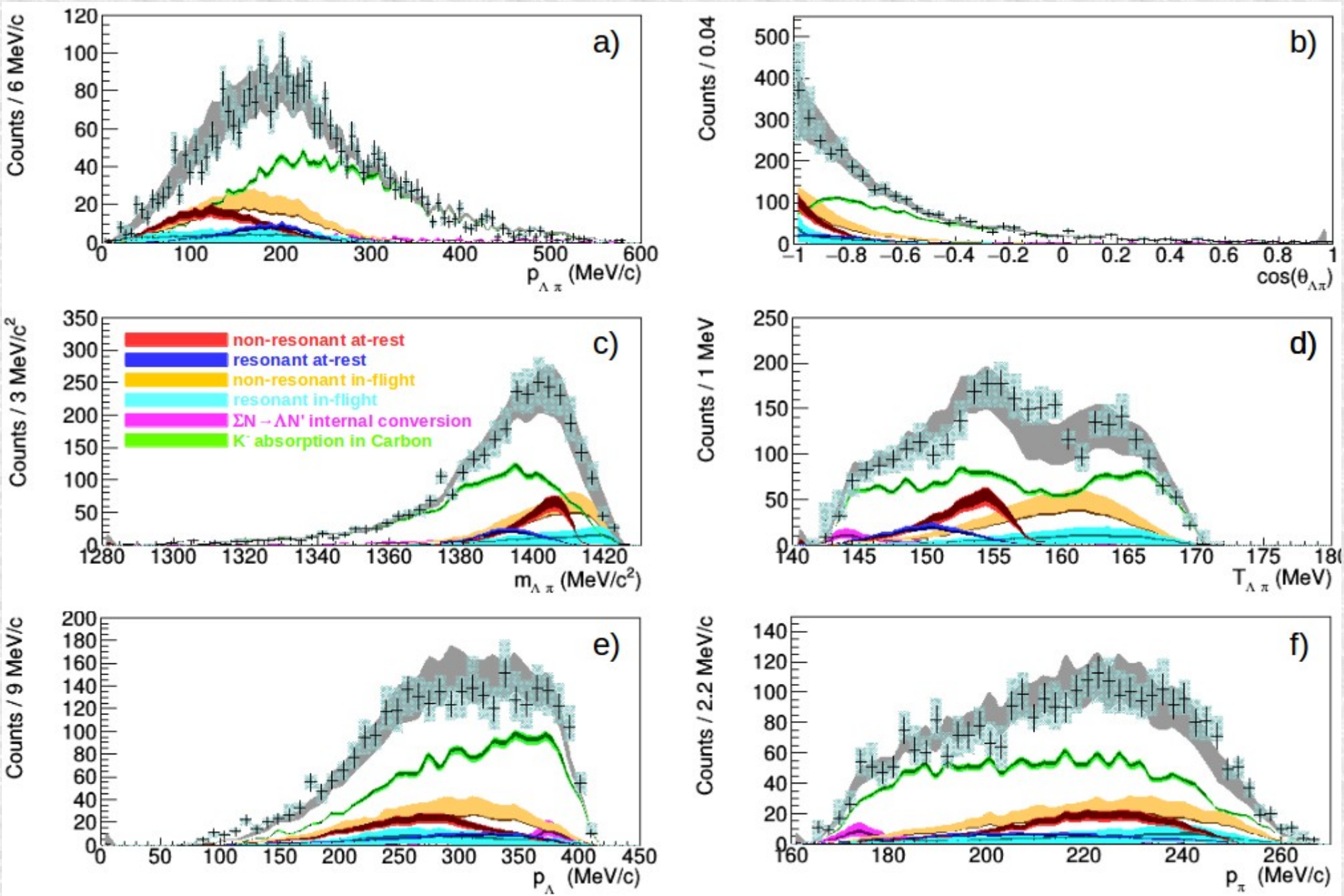

Comparison

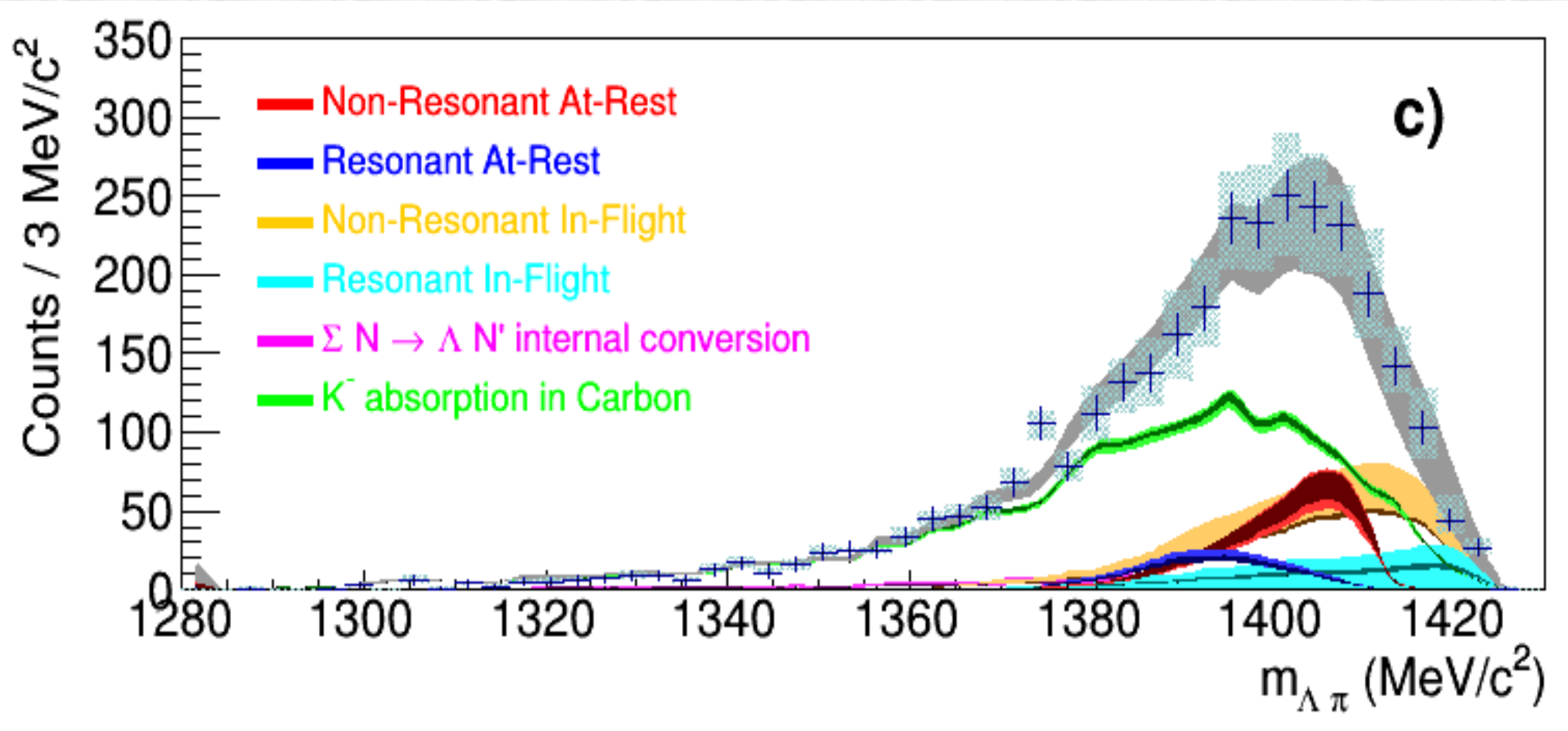

$m_{\Lambda\pi}$ fit

Light band sys err.
Dark band stat. Err.

Outcome of the measurement

From the well known Σ* transition probability:

$$\frac{\mathrm{NR-ar}}{\mathrm{RES-ar}} = \frac{\int_0^{pmax} P_{ar}^{nr}(p_{\Lambda\pi})\, dp_{\Lambda\pi}}{\int_0^{pmax} P_{ar}^{res}(p_{\Lambda\pi})\, dp_{\Lambda\pi}} =$$

$$= |f_{ar}^{s}|^2 \cdot 8,94 \cdot 10^5 \mathrm{MeV}^2 \,.$$

$$\Downarrow$$

$$|f_{ar}^{nr}| = |A_{K-n\to\Lambda\pi^-}| = (0.334 \pm 0.018\,\mathrm{stat}^{+0.034}_{-0.058}\mathrm{syst})\ \mathrm{fm}$$

compatible with K^- p → Λ π^0 scattering above threshold

J. K. Kim, Columbia University Report, Nevis 149 (1966),

J. K. Kim, Phys Rev Lett, 19 (1977) 1074:

$E = -33$ MeV	$p_{lab} = 120$ MeV	160 MeV	200 MeV	245 MeV
$0.334 \pm 0.018\,\mathrm{stat}^{+0.034}_{-0.058}\mathrm{syst}$	0.33(11)	0.29(10)	0.24 (6)	0.28(2)

Outcome of the measurement

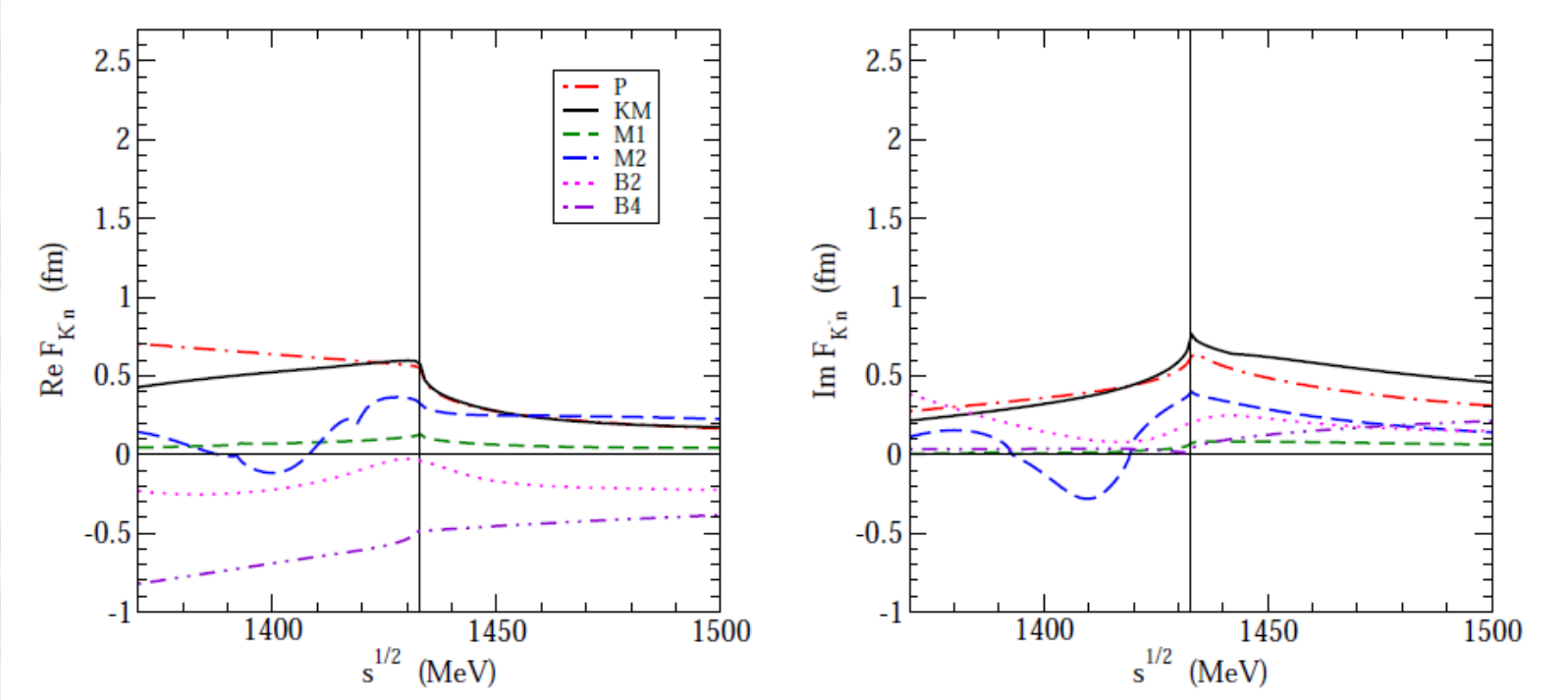

To compare with theoretical calculations:

1) extract the amplitude for each model .. $A_{K\text{-}n} = (\mathrm{ReF}^2_{K\text{-}n} + \mathrm{ImF}^2_{K\text{-}n})^{1/2}$

2) scale the amplitudes for the K^- **n couplings to the** $\Sigma^-\pi^0$ **and** $\Sigma^0\pi^-$ **channels:**

$$\frac{Prob_{K^-n\to\Lambda\pi^-}}{Prob_{K^-n\to\Sigma^-\pi^0}} = \frac{Ph_{K^-n\to\Lambda\pi^-}}{c_1 Ph_{K^-n\to\Sigma^-\pi^0}}$$

Isospin $(I, I_z) =$
$= (1, -1)$ **component**

$$\frac{Prob_{K^-n\to\Lambda\pi^-}}{Prob_{K^-n\to\Sigma^0\pi^-}} = \frac{Ph_{K^-n\to\Lambda\pi^-}}{c_2 Ph_{K^-n\to\Sigma^0\pi^-}}$$

Phase spaces ratios

comparison with th. models

$$|f^s_{ar}| = (0.334 \pm 0.018\,\mathrm{stat}^{+0.034}_{-0.058}\mathrm{syst})\ \mathrm{fm}\,.$$

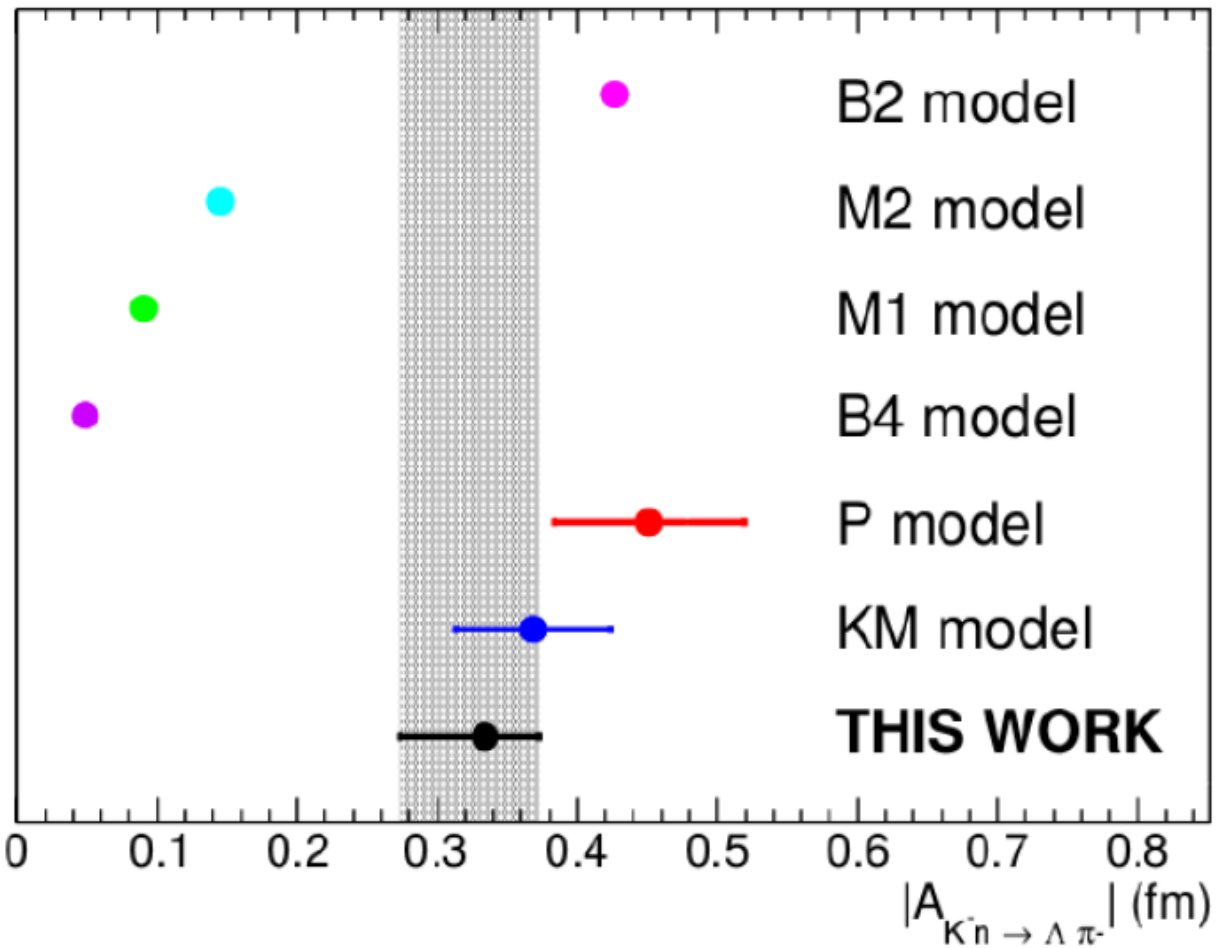

$A_{K\text{-}n \to \Lambda\pi}$ $(s^{1/2} \sim 1400\ \mathrm{MeV})^{1/2}$

$$E_{Kn} = -|B_n| - \frac{p_3^2}{2\mu_{\pi,\Lambda,3He}}$$

Nucl. Phys. A954 (2016) 75-93

Phys. Rev. C 96 (2017) 045204

Phys. Lett. B 702 (2011) 402-407

Nucl.Phys. A968 (2017) 35-47

K. P., S. Wycech, L. Fabbietti et al. Phys.Lett. B782 (2018) 339-345

comparison with th. models

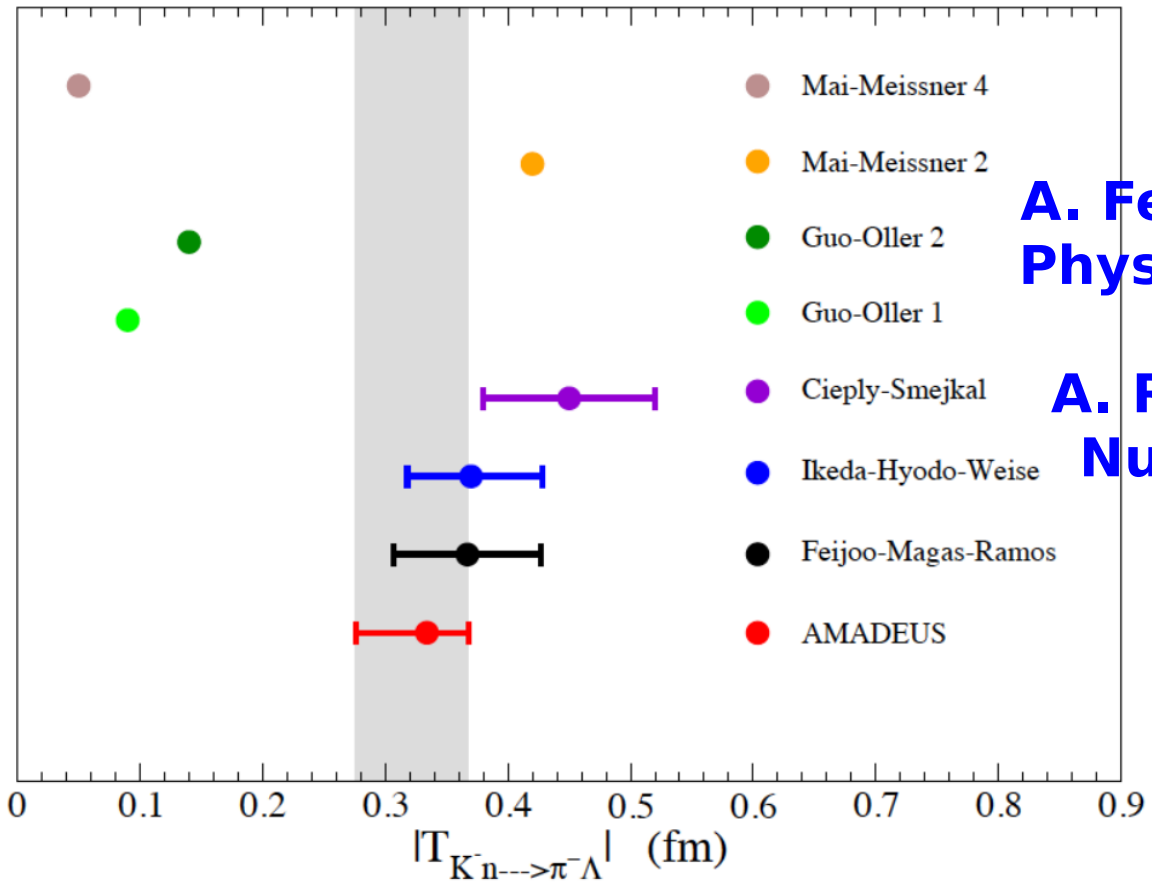

See talk by A. Ramos

A. Feijoo, V.K. Magas, A. Ramos, Phys. Rev. C92 (2015) 1, 015206

A. Ramos, A. Feijoo, V. Magas, Nucl. Phys. A 954, 58 (2016)

K^- - multiN absorption and search for bound states

AMADEUS contribution from low energy $K^{-}\ ^{12}C$ absorption $\Sigma^0 p$ / Λp final states

O. Vazquez Doce et al, Phys Lett B 758, (2016) 134

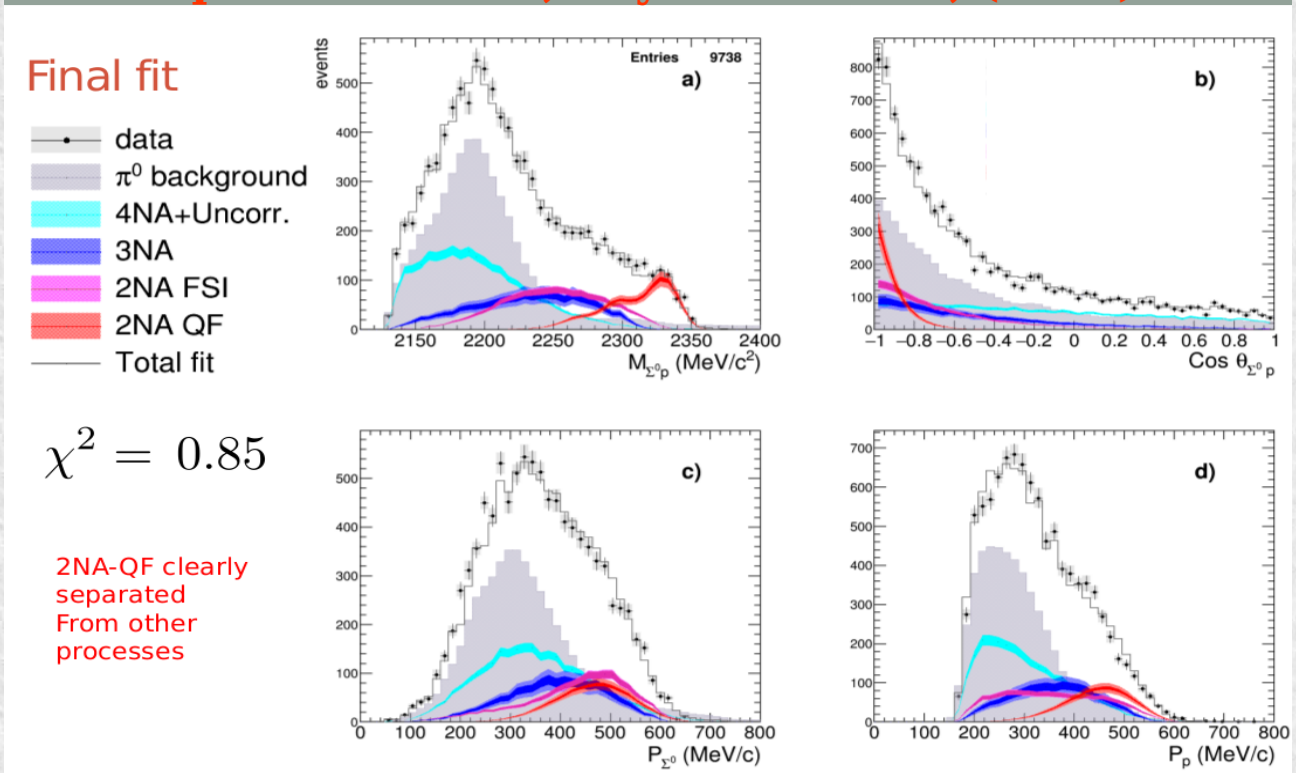

From the contributions to the fit, the yields are extracted for K- stop

	yield / $K^-_{stop} \cdot 10^{-2}$	$\sigma_{stat} \cdot 10^{-2}$	$\sigma_{syst} \cdot 10^{-2}$
2NA-QF	0.127	$\pm$ 0.019	$^{+0.004}_{-0.008}$
2NA-FSI	0.272	$\pm$ 0.028	$^{+0.022}_{-0.023}$
Tot 2NA	0.376	$\pm$ 0.033	$^{+0.023}_{-0.032}$
3NA	0.274	$\pm$ 0.069	$^{+0.044}_{-0.021}$
Tot 3body	0.546	$\pm$ 0.074	$^{+0.048}_{-0.033}$
4NA + bkg.	0.773	$\pm$ 0.053	$^{+0.025}_{-0.076}$

no significant bound state emerges at the level of 2σ

- **Λp analogous analysis finalized**
- **K-multi-nucleon yields & cross sections obtained for pK ~ 100 MeV/c**
- **disappearance of the bound state in $K^-\ ^{12}C$ induced reaction explained**

AMADEUS contribution from low energy K^- ^{12}C absorption $\Sigma^0 p$ / Λp final states

Simultaneous fit of:

- Λp invariant mass;
- angular correlation;
- proton momentum;
- Λ momentum.

Total reduced χ^2 :

$\chi^2/dof = 0.94$

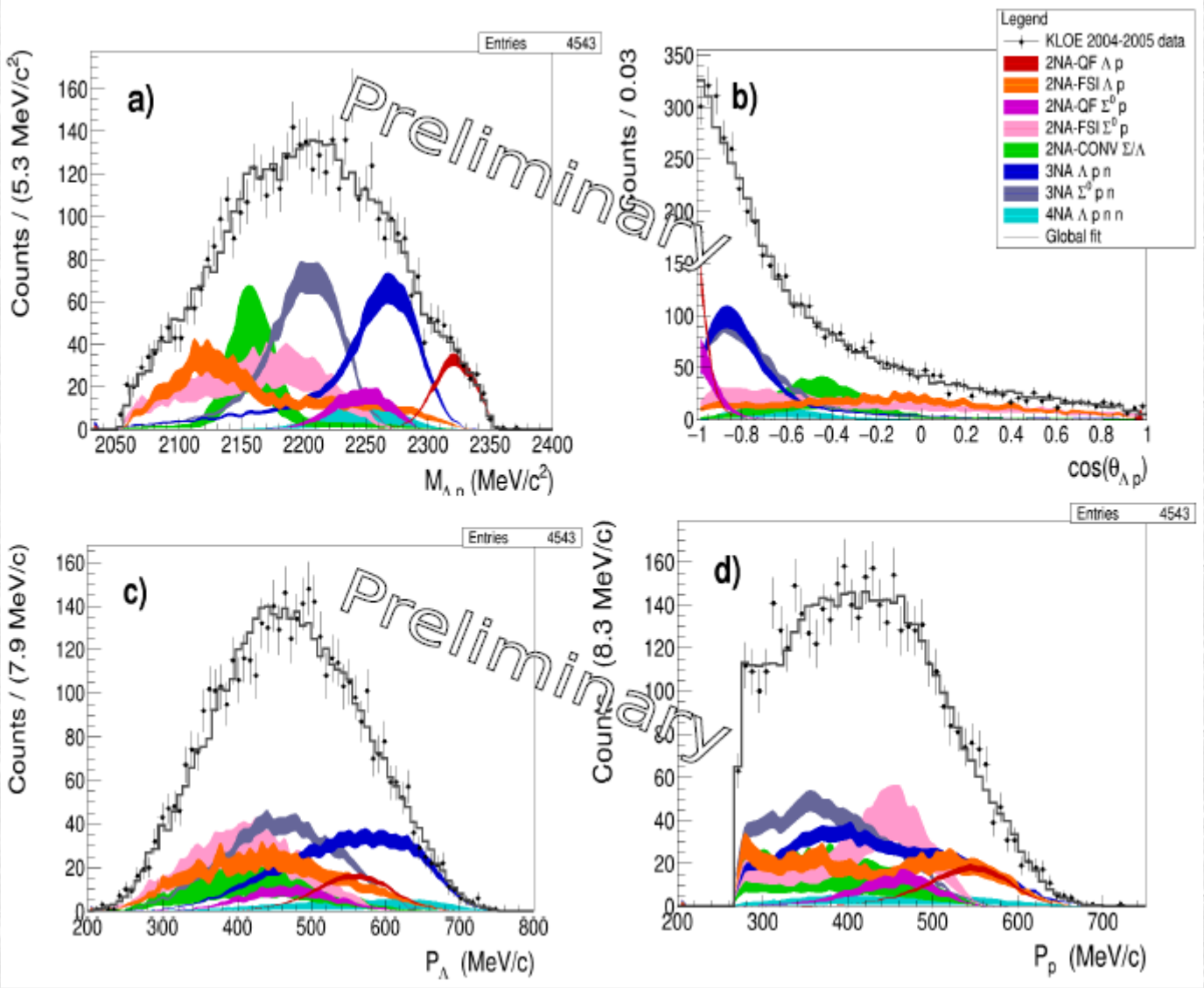

AMADEUS contribution from low energy K^- ^{12}C absorption $\Sigma^0 p$ / Λp final states

Table 1 Branching ratios and cross sections of the K^- multi-nucleon absorption processes. The statistical and systematic errors are also shown.

Process	Banching Ratio (%)	σ (mb)	@	p_K (MeV/c)
2NA-QF Λp	0.25 ± 0.02 (stat.) $^{+0.01}_{-0.02}$(syst.)	2.8 ± 0.3 (stat.) $^{+0.1}_{-0.2}$ (syst.)	@	128 ± 29
2NA-FSI Λp	6.2 ± 1.4(stat.) $^{+0.5}_{-0.6}$(syst.)	69 ± 15 (stat.) ± 6 (syst.)	@	128 ± 29
2NA-QF Σ^0p	0.35 ± 0.09(stat.) $^{+0.13}_{-0.06}$(syst.)	3.9 ± 1.0 (stat.) $^{+1.4}_{-0.7}$ (syst.)	@	128 ± 29
2NA-FSI Σ^0p	7.2 ± 2.2(stat.) $^{+4.2}_{-5.4}$(syst.)	80 ± 25 (stat.) $^{+46}_{-60}$ (syst.)	@	128 ± 29
3NA Λpn	1.4 ± 0.2(stat.) $^{+0.1}_{-0.2}$(syst.)	15 ± 2 (stat.) ± 2 (syst.)	@	117 ± 23
3NA Σ^0pn	3.7 ± 0.4(stat.) $^{+0.2}_{-0.4}$(syst.)	41 ± 4 (stat.) $^{+2}_{-5}$ (syst.)	@	117 ± 23
4NA Λpnn	0.13 ± 0.09(stat.) $^{+0.08}_{-0.07}$(syst.)	-		
2NA-Σ/Λconv.	2.1 ± 1.2(stat.) $^{+0.9}_{-0.5}$(syst.)	-		

Preliminary

The ratio between the branching ratios of the 2NA-QF in the Λp channel and in the Σ^0p is measured to be:

$$\mathcal{R} = 0.7 \pm 0.2(\text{stat.})^{+0.2}_{-0.3}(\text{syst.})$$

Preliminary

and the ratio between the corresponding phase spaces is 1.22 .
According to the pion exchange model:

$$\mathcal{R} = \frac{\text{BR}(K^- pp \to \Lambda p)}{\text{BR}(K^- pp \to \Sigma^0 p)} = \frac{\text{BR}(K^- p \to \Lambda \pi^0)}{\text{BR}(K^- p \to \Sigma^0 \pi^0)}$$

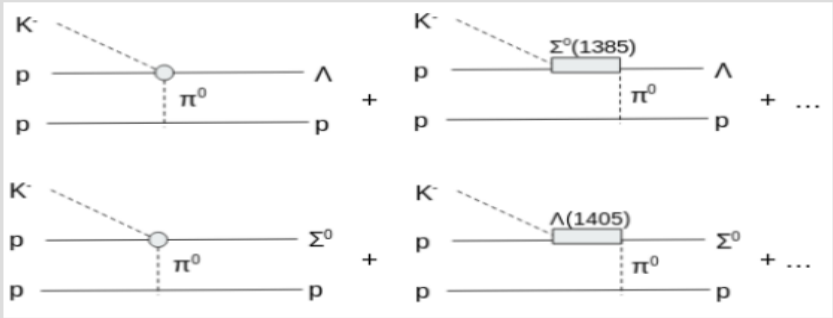

AMADEUS contribution from low energy K^- ^{12}C absorption $\Sigma^0 p$ / Λp final states

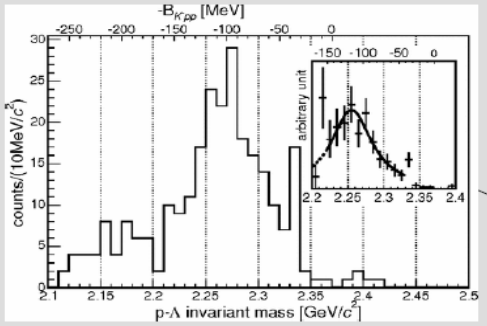

FINUDA: $K^-_{stop} + X \rightarrow \Lambda + p + X'$

[M. Agnello et al., Phys. Rev. Lett. 94, 212303 (2005)]

6 targets: - 3 of ^{12}C (50%)
- 2 of ^6Li (35%)
- 1 of ^7Li (15%)

Interpreted as the signal of:
$K^-pp \rightarrow \Lambda + p$

1. **But...the large number of events originates from K^- absorption on ^{12}C**
2. **only back-to-back Λp pairs ($\cos\theta_{\Lambda p} < -0.8$)**

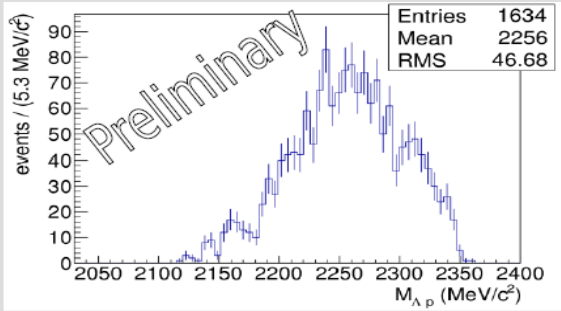

$K^- + {}^{12}C \rightarrow \Lambda + p + R$

Measured spectra **but only back-to-back Λp events** a la FINUDA **($\cos\theta_{\Lambda p} < -0.8$)**

→ the shape of the Λp invariant mass spectrum is compatible with the spectrum reported by FINUDA

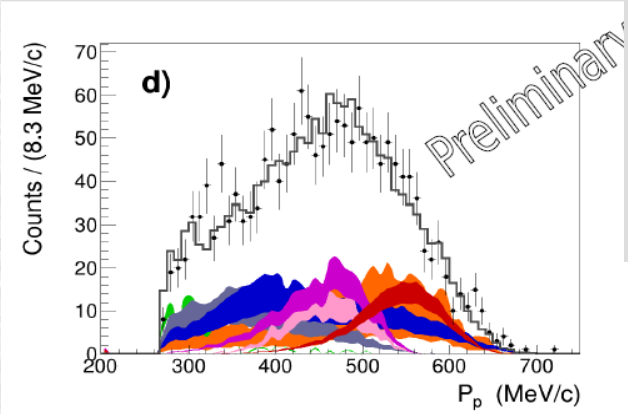

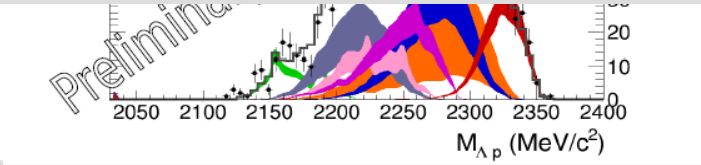

Simultaneous fit of:

- Λp invariant mass;
- angular correlation;
- proton momentum;
- Λ momentum.

Total reduced χ^2:

$\chi^2/dof = 0.94$

Process	Branching Ratio (%)
2NA-QF Λp	$0.20 \pm 0.04(\text{stat.}) \pm 0.02(\text{syst.})$
2NA-FSI Λp	$3.8 \pm 2.3(\text{stat.}) \pm 1.1(\text{syst.})$
2NA-QF $\Sigma^0 p$	$0.54 \pm 0.20(\text{stat.})\ ^{+0.20}_{-0.16}(\text{syst.})$
2NA-FSI $\Sigma^0 p$	$5.4 \pm 1.5(\text{stat.})\ ^{+1.0}_{-2.7}(\text{syst.})$
3NA Λpn	$1.1 \pm 0.3(\text{stat.}) \pm 0.2(\text{syst.})$
3NA $\Sigma^0 pn$	$1.9 \pm 0.7(\text{stat.})\ ^{+0.8}_{-0.4}(\text{syst.})$
2NA-Σ/Λconv	$22 \pm 4(\text{stat.})\ ^{+1}_{-12}(\text{syst.})$

Preliminary

AMADEUS contribution from low energy K^- ^{12}C absorption $\Sigma^0 p$ / Λp final states

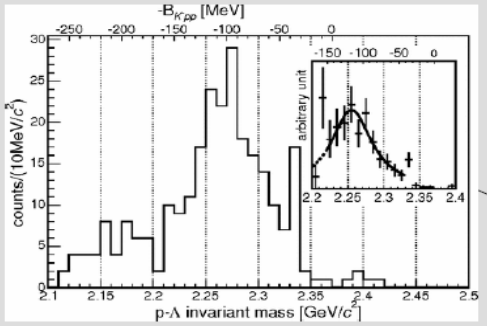

FINUDA: $K^-_{stop} + X \rightarrow \Lambda + p + X'$

[M. Agnello et al., Phys. Rev. Lett. 94, 212303 (2005)]

6 targets: - 3 of ^{12}C (50%)
- 2 of ^6Li (35%)
- 1 of ^7Li (15%)

Interpreted as the signal of:
$K^-pp \rightarrow \Lambda + p$

1. But...the large number of events originates from K^- absorption on ^{12}C
2. only back-to-back Λp pairs ($\cos\theta_{\Lambda p} < -0.8$)

→ Λ + p + R

d spectra **but only back-to-back Λp events** a la
($\cos\theta_{\Lambda p} < -0.8$)

ape of the Λp invariant mass spectrum is
ble with the spectrum reported by FINUDA

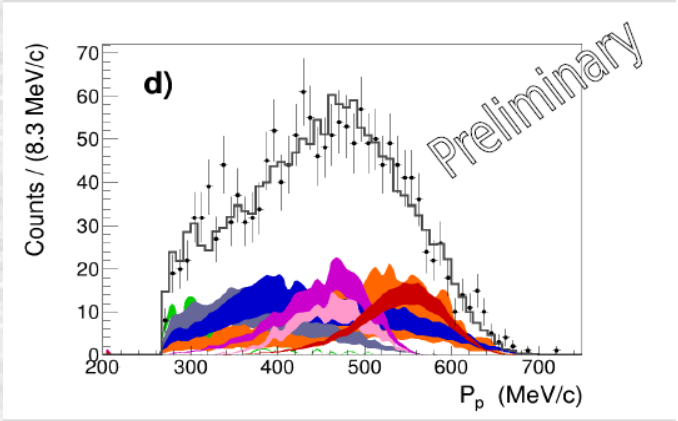

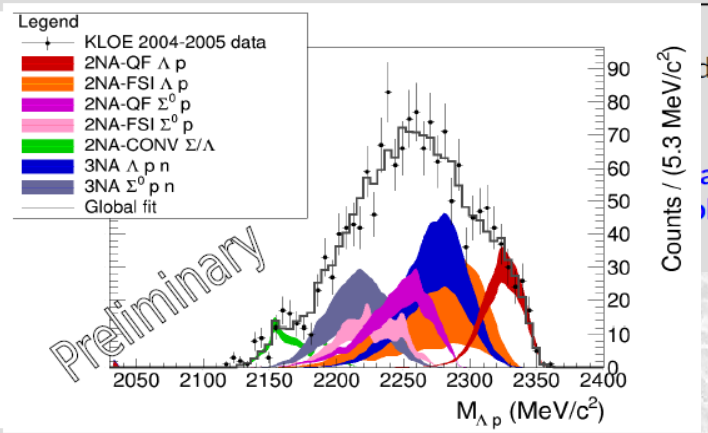

Simultaneous fit of:

- Λp invariant mass;
- angular correlation;
- proton momentum;
- Λ momentum.

Total reduced χ^2:

$\chi^2/dof = 0.94$

Process	Branching Ratio (%)
2NA-QF Λp	$0.20 \pm 0.04(\text{stat.}) \pm 0.02(\text{syst.})$
2NA-FSI Λp	$3.8 \pm 2.3(\text{stat.}) \pm 1.1(\text{syst.})$
2NA-QF Σ^0p	$0.54 \pm 0.20(\text{stat.})\ ^{+0.20}_{-0.16}(\text{syst.})$
2NA-FSI Σ^0p	$5.4 \pm 1.5(\text{stat.})\ ^{+1.0}_{-2.7}(\text{syst.})$
3NA Λpn	$1.1 \pm 0.3(\text{stat.}) \pm 0.2(\text{syst.})$
3NA Σ^0pn	$1.9 \pm 0.7(\text{stat.})\ ^{+0.8}_{-0.4}(\text{syst.})$
2NA-Σ/Λconv	$22 \pm 4(\text{stat.})\ ^{+1}_{-12}(\text{syst.})$

Preliminary

K^- - 4NA cross section & BR

Λt available data

Available data:

- in Helium :

  - bubble chamber experiment
  [M.Roosen, J.H. Wickens, Il Nuovo Cimento 66, (1981), 101]
  K^- stopped in liquid helium, Λ dn/t search. 3 events compatible with the Λt kinematics were found

  BR($K^{-4}He \rightarrow \Lambda t$) **= (3 ± 2) × 10^{-4} /K_{stop}** global, no 4NA

- Solid targets

  - FINUDA [Phys.Lett. B669 (2008) 229]
  (40 events in different solid targets)

Λt available data

FINUDA presented [Phys.Lett.B (2008) 229]:

- a study of Λ vs t momentum correlation and an opening angle distribution
- **40 events** collected and added together coming from different targets (^{6,7}Li, ^{9}Be)

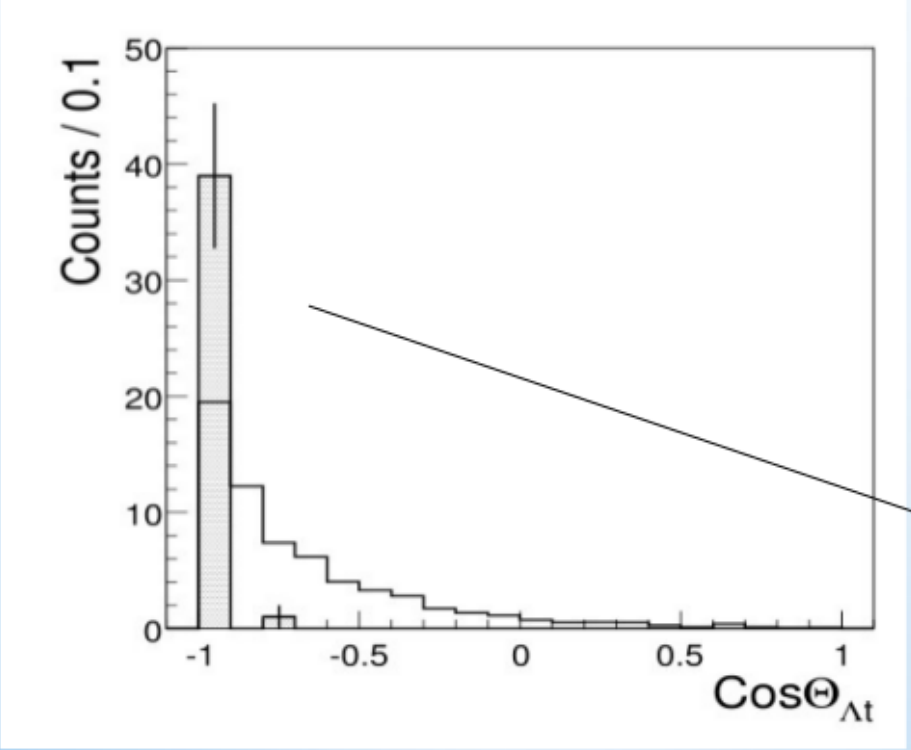

Filled histogram= data

Open histogram = Phase space simulation

K- A → Λ t A'

Unclear back to back topology

Λt emission yield → 10^{-3} – 10^{-4} / K^{-}_{stop}

global, no 4NA

Experimental data only back-to-back

$K^- \ ^4He \rightarrow \Lambda t$ cross section, DC gas sample contributing processes:

single nucleon absorption (1NA)

$$K^- \ ^4He \rightarrow \Lambda \ \pi^0 \ t_{res}$$

$$K^- \ ^4He \rightarrow \Sigma^0 \pi^0 \ t_{res} \quad , \quad \Sigma^0 \rightarrow \Lambda \gamma$$

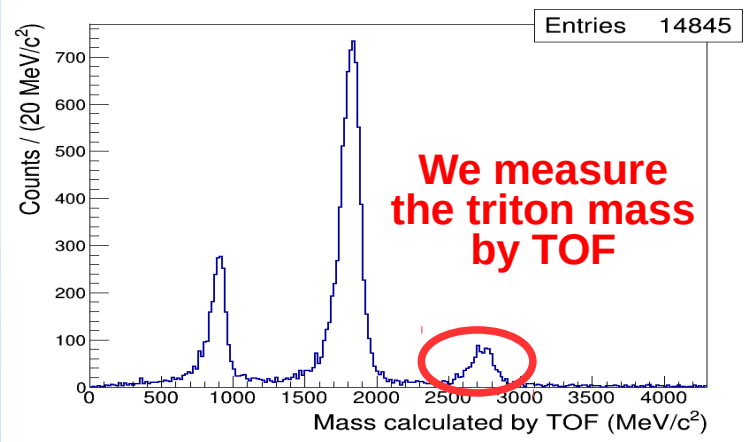

Spectator tritons have low momentum:

p_t ~ Fermi momentum

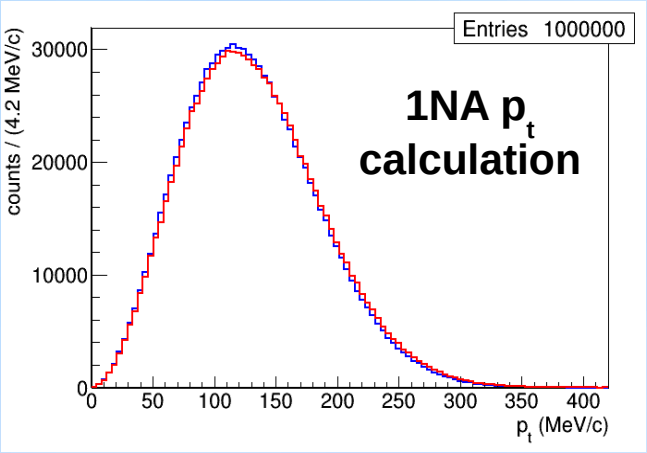

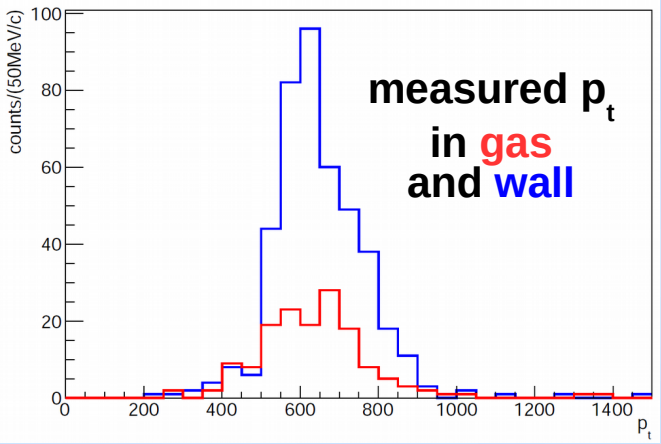

4NA processes – K^- absorbed on FREE α:

- $K^- \ ^4He \rightarrow \Lambda t$
- $K^- \ ^4He \rightarrow \Sigma^0 t \quad , \quad \Sigma^0 \rightarrow \Lambda \gamma$

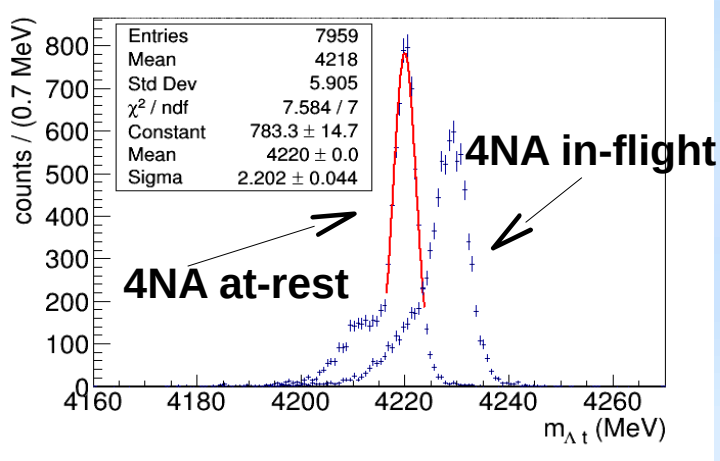

$K^-\ {}^4He \rightarrow \Lambda t$ cross section, DC gas sample contributing processes:

Main background: K^- absorption on ^{12}C (isobutane contamination)

4NA: $K^-\ {}^{12}C \rightarrow K^-\ (\alpha)^{bound}\ {}^8Be \rightarrow \Lambda/\Sigma^0\ t\ {}^8Be$

7 MeV/c^2 lower invariant mass threshold respect to:

4NA: $K^-\ {}^4He \rightarrow K^-\ (\alpha)^{free} \rightarrow \Lambda/\Sigma^0\ t$

+

all possible elastic/inelastic FSI processes with primary Λ/Σ formation

uncorrelated Λt low invariant mass:

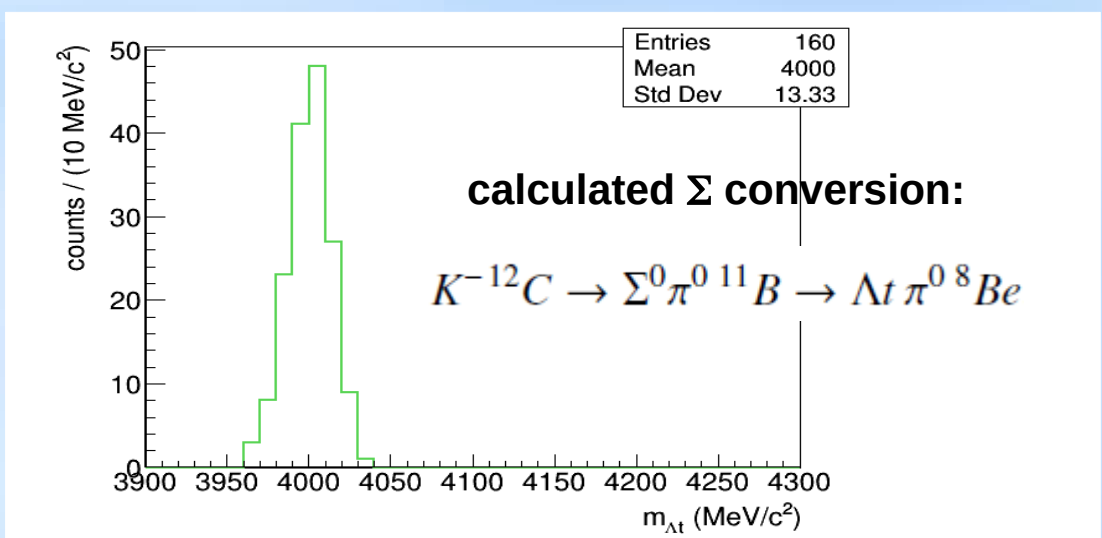

Measured $K^-\ {}^{12}C$ sample from K- captures in wall:

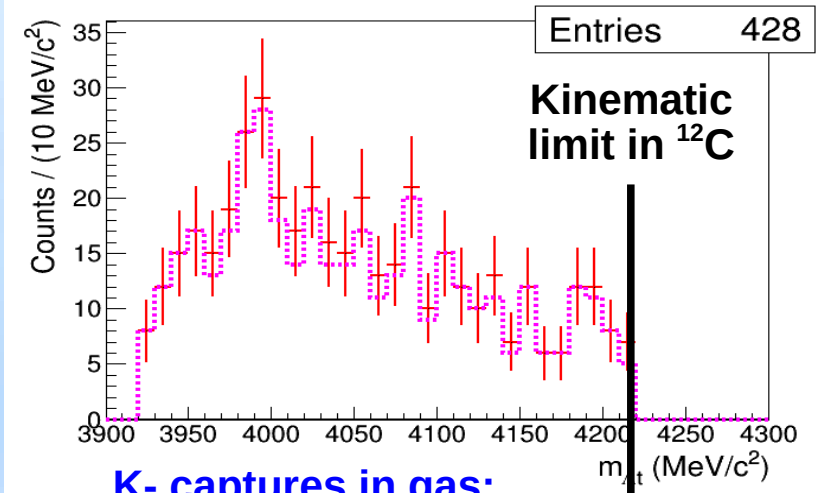

K- captures in gas:

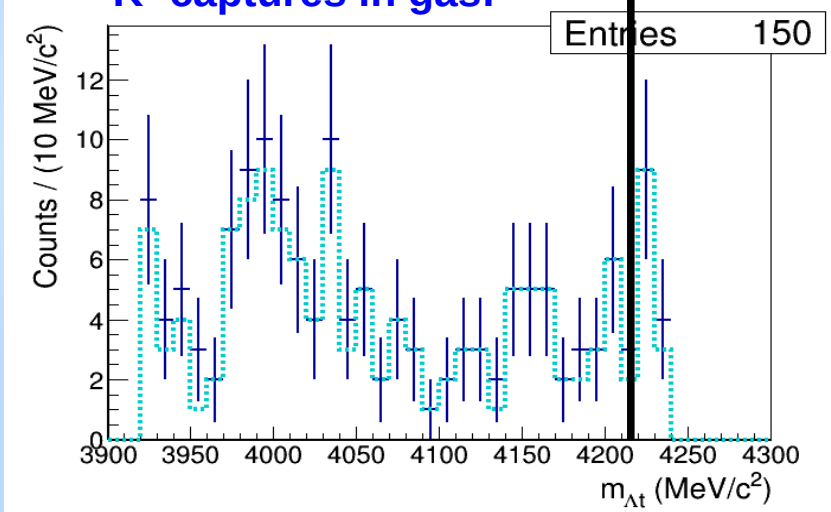

K- ^{4}He → Λt 4NA fit

preliminary

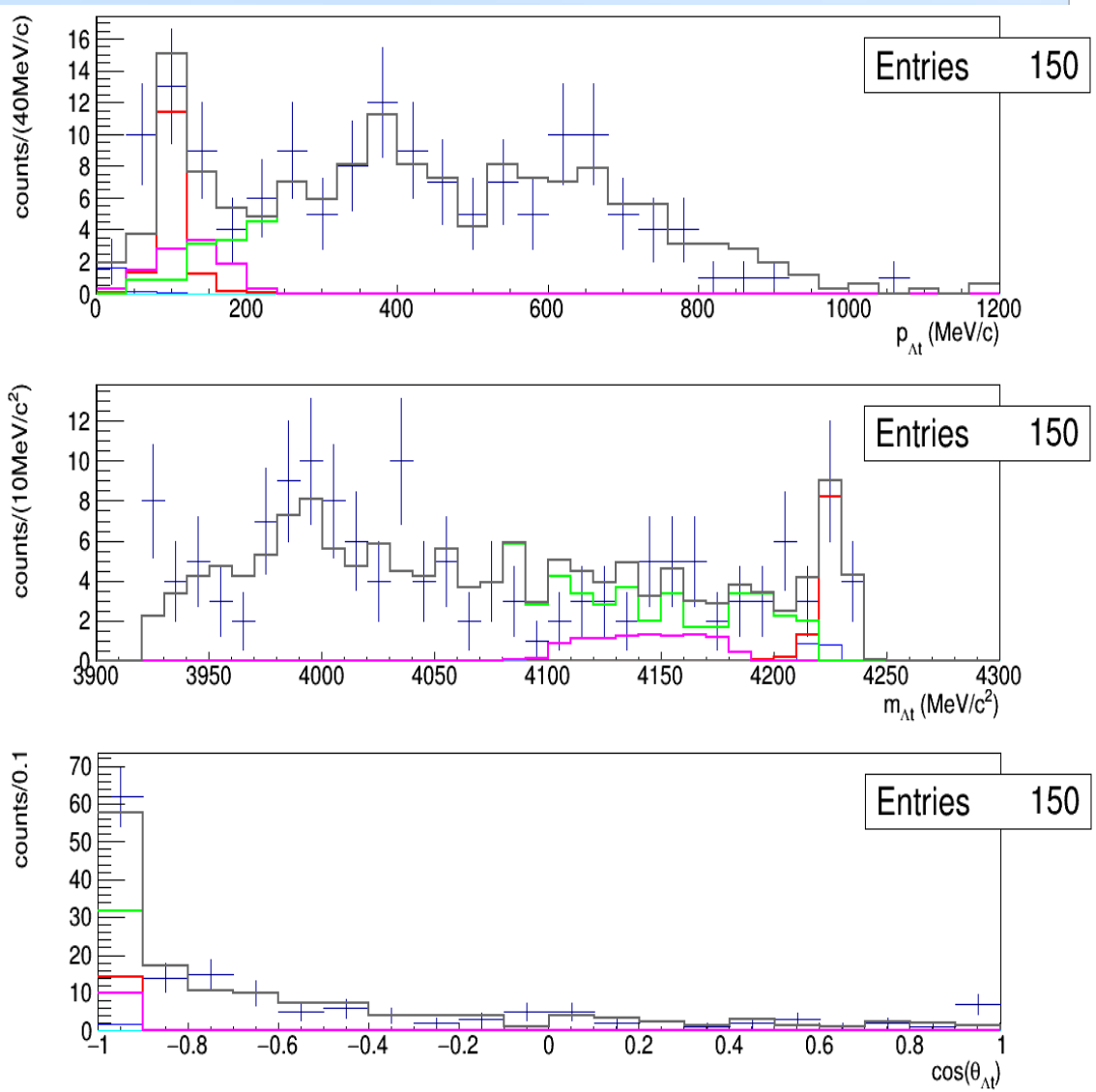

data

--- carbon data from DC wall

--- 4NA K$^-$ ^{4}He → Λt in flight MC

--- 4NA K$^-$ ^{4}He → Λt at rest MC

--- 4NA K$^-$ ^{4}He → Σ^0t , Σ^0 → Λγ MC

--- 4NA K$^-$ ^{4}He → Σ^0t , Σ^0 → Λγ MC

K- ^{4}He → Λt 4NA fit

BR(K^{-4}He(4NA) → Λt) **< 2.0 × 10^{-4} /K_{stop} (95% c. l.)**

σ(100 **± 19** MeV/c) (K^{-4}He(4NA) → Λt) **=**
= (0.81 ± 0.21 (stat) $^{+0.03}_{-0.04}$ (syst)) mb

preliminary

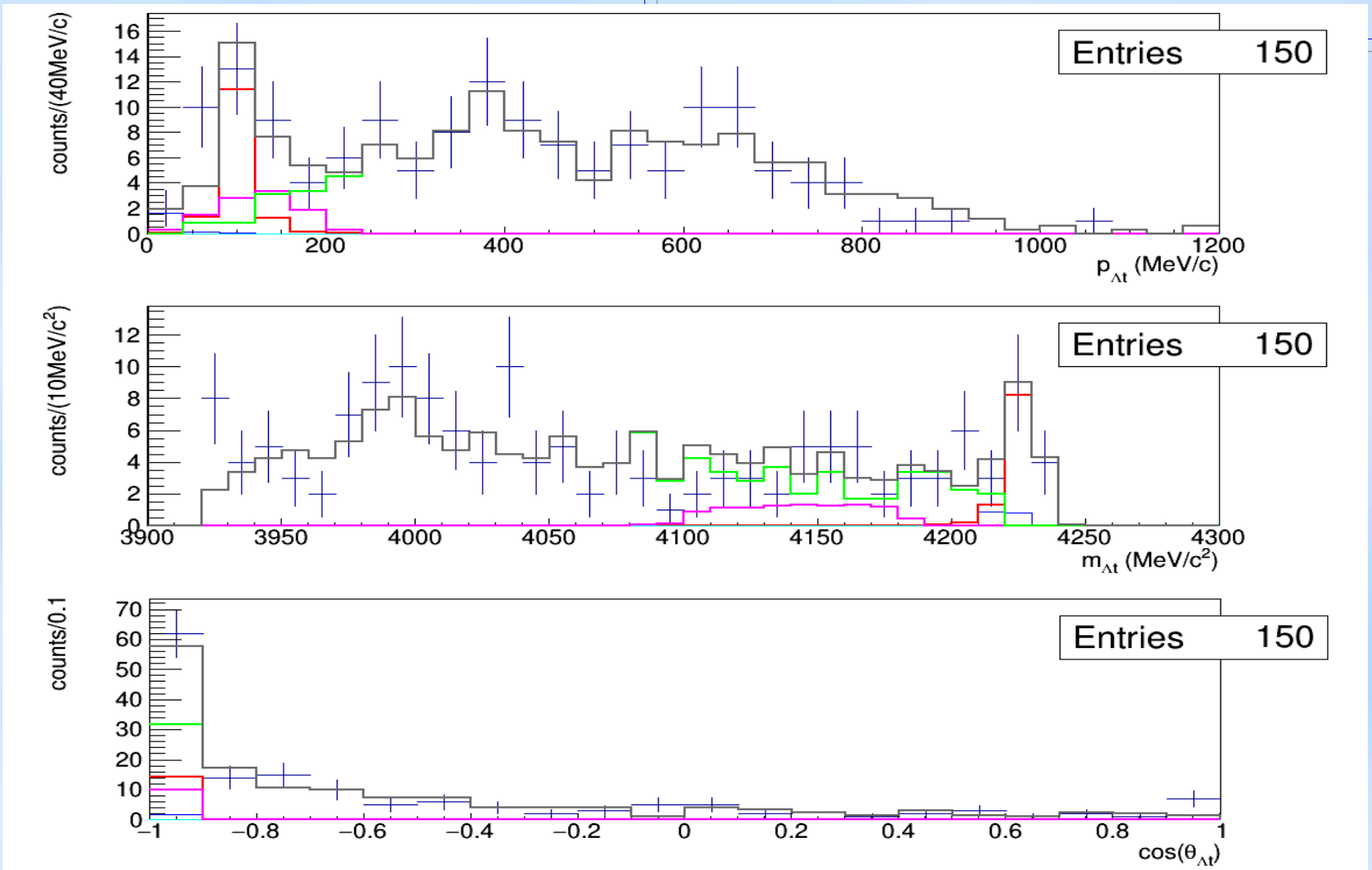

K- ^{12}C → Λ/Σ^0 t ^{8}Be 4NA without FSI

preliminary

BR(K^{-4}He(4NA) → Λt) = **1.5 ± 0.5 × 10^{-4} (stat) $^{+0.7 \times 10\text{-}4}_{-0.3 \times 10\text{-}4}$ (syst) /K_{stop}**

σ(K^{12}C (4NA) → Λt ^{8}Be) = **0.58 ± 0.11 (stat) $^{+0.03}_{-0.10}$ (syst) mb**

σ(K^{12}C (4NA) → Σ^{0}t ^{8}Be) = **1.88 ± 0.35 (stat) $^{+0.21}_{-0.21}$ (syst) mb**

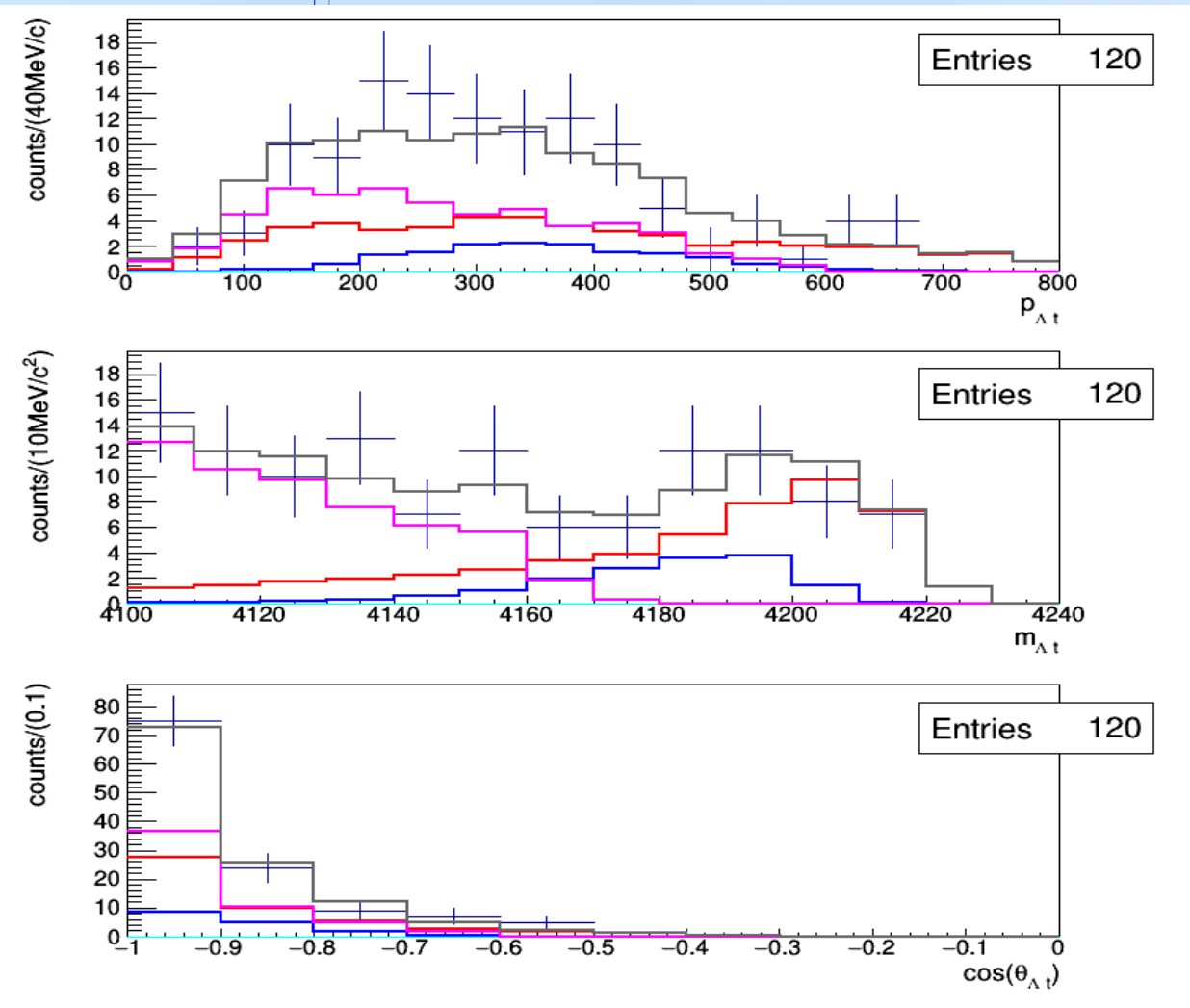

Perspective:

Measurement of the

$K^- H \rightarrow \Sigma^0\pi^0$ cross section for $p_K = 97 \pm 10$ MeV/c

Y. Ikeda, T. Hyodo, W. Weise,
PLB 706, 63 (2011); NPA 881 98 (2012)

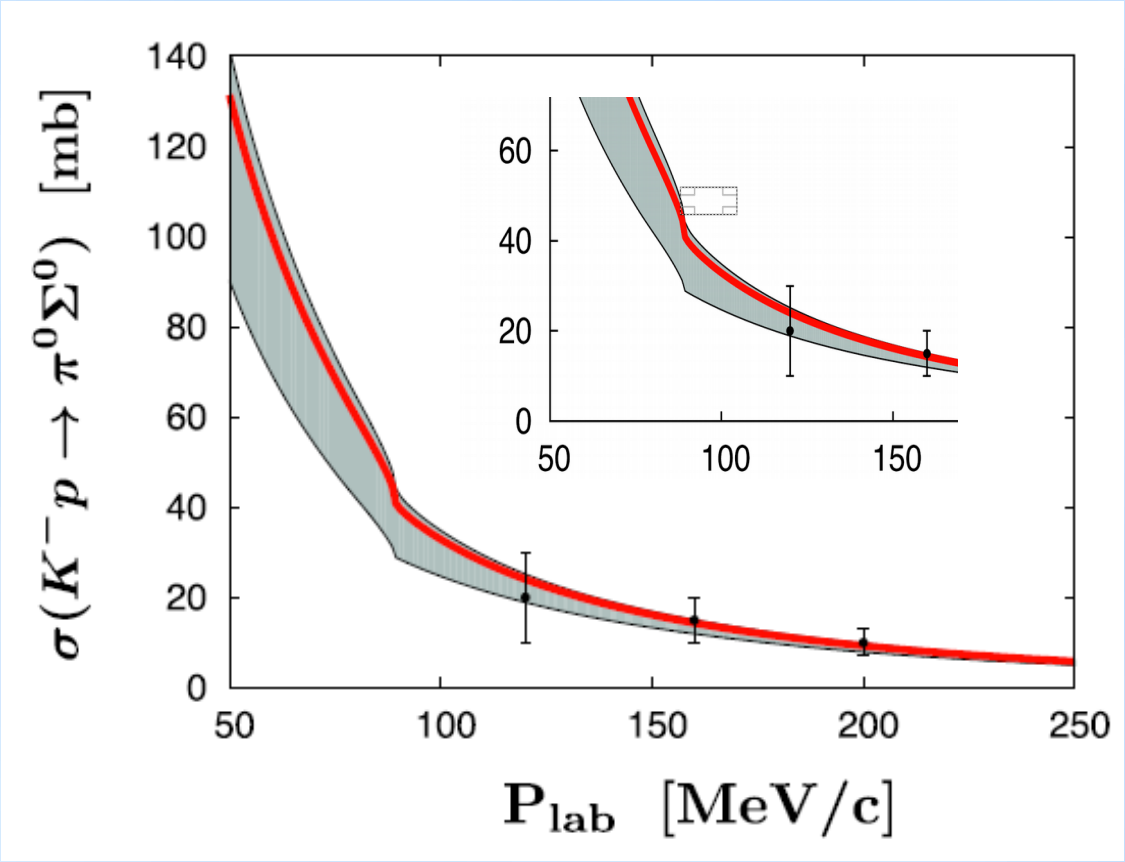

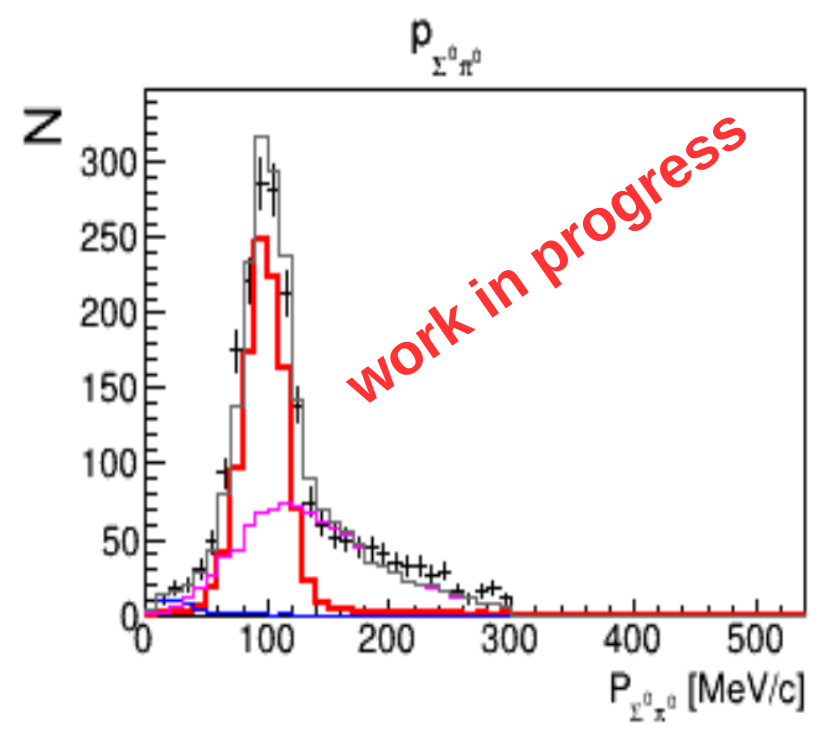

Low momentum p_{Σ^+} structure in $\Sigma^+\pi^-$ formation

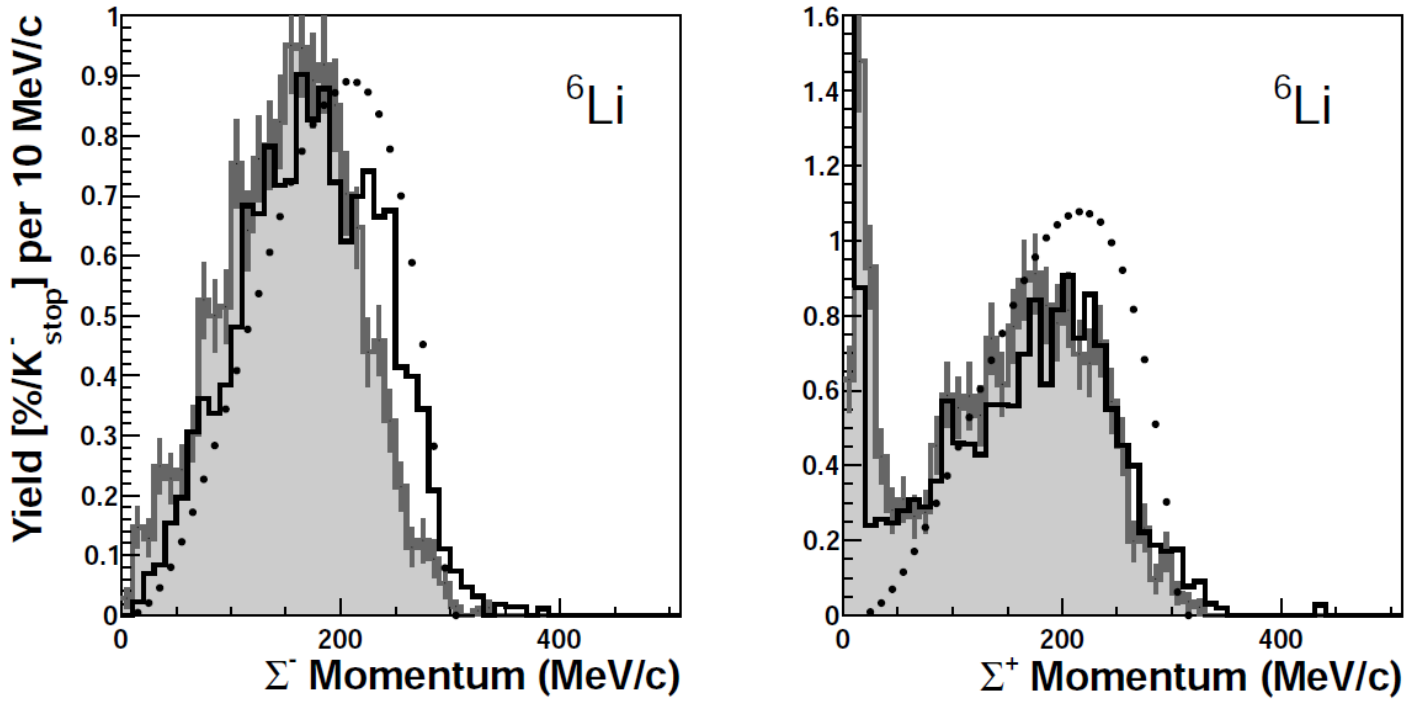

Fig. 5. Momentum distributions of sigmas from the $^6Li(K^-_{stop}, \pi^\pm\Sigma^\mp)A'$ reactions. The grey-filled histograms are the measured distributions. The distributions of Monte-Carlo generated sigmas are depicted by full dots, and with open diagrams are represented the M-C generated sigmas being reconstructed by FINUDA.

FINUDA coll. M. Agnello et al., Phys. Lett. B704 (2011) 474.

K^- ^6Li → $\Sigma^+\pi^-$ A'

Gamov state formation of a Σ^+ in light nuclei?

K. Piscicchia et al., EPJ Web Conf. 137 (2017) 09005.

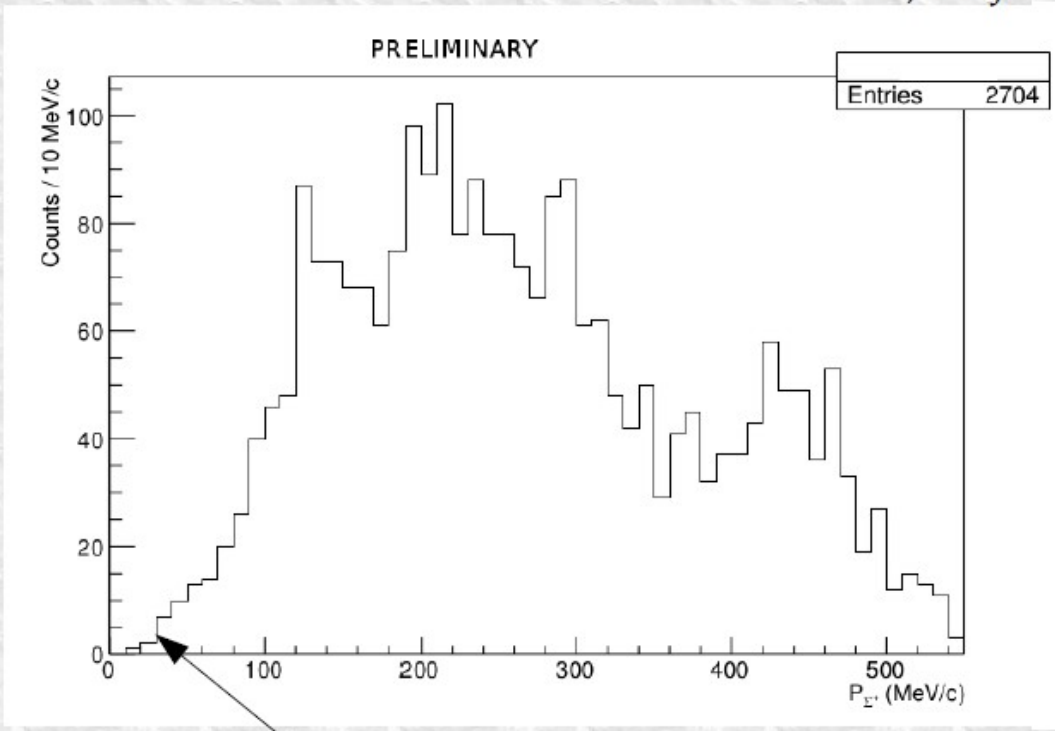

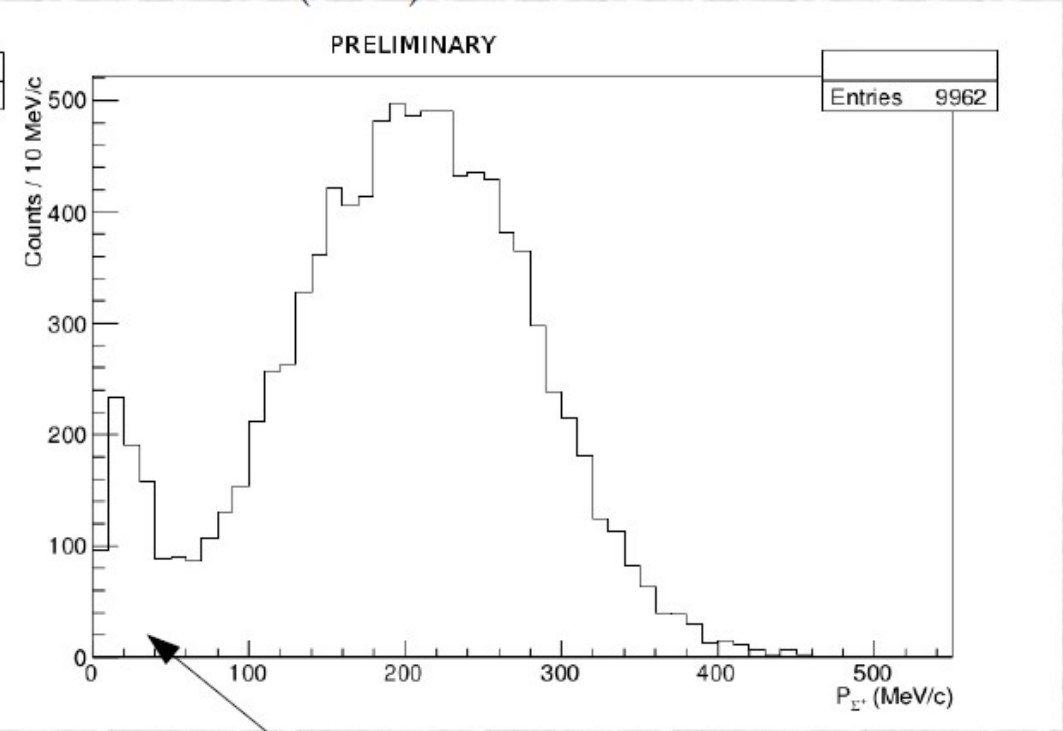

$K^- \, {}^9Be \rightarrow \Sigma^+\pi^- + \alpha + n + t$

no structure at low momentum

$K^- \, {}^{12}C \rightarrow \Sigma^+\pi^- \, A'$

structure at low momentum

can not be explained by energy loss, the target is much thiner

Low momentum p_{Σ^+} structure in $\Sigma^+\pi^-$ formation

K. Piscicchia et al., EPJ Web Conf. 137 (2017) 09005.

$K^- \, {}^9Be \rightarrow \Sigma^+\pi^- + + \alpha + n + t$

no structure at low momentum

$K^- \, {}^{12}C \rightarrow \Sigma^+\pi^- \, A'$

structure at low momentum

amounts some % of the total yield

also in thiner targets

(not explained by energy loss)

Hypothesis: Σ^+ trapped in a Gamov state, interplay of the attractive nuclear potential & repulsive Coulomb barrier

S. Wycech, K. P., EPJ Web. Conf. 130 (2016) 02011

R. Del Grande, K. P. and S. Wycech, Acta Phys.Polon. B48 (2017) 1881

S. Wycech, K. P., On Gamov states of Σ^+ hyperons, Acta Phys.Polon. B48 (2017) 1861

Gamov state formation of a Σ^+ in light nuclei?

… work in progress

Gamov peak following in-flight capture

$K^- \ ^{12}C \rightarrow \Sigma^+\pi^- \ ^{11}Be$

about 3% of the large peak

Breit – Wigner - (E, Γ) = (1405,40) ; (1410,40) ; (1420,40)

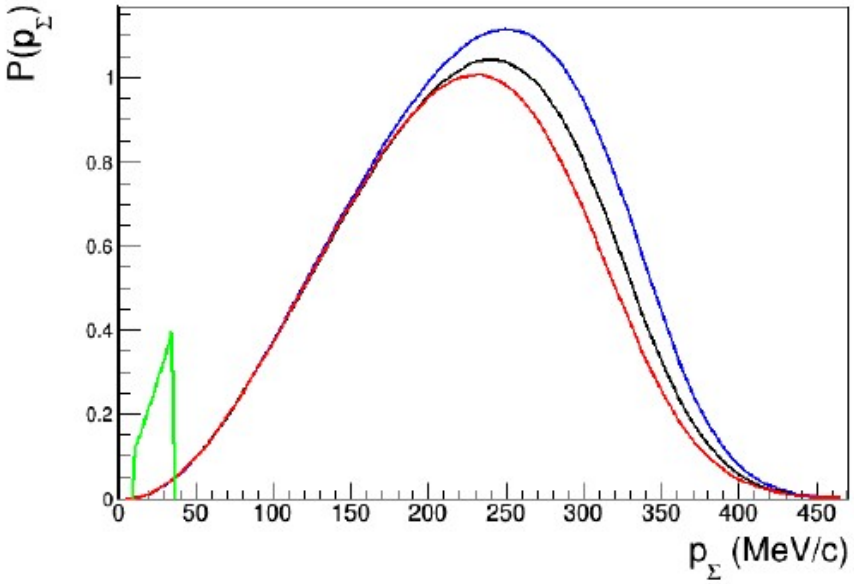

Position $p_{\Sigma+}$ = 15 MeV/c

peculiar structure due to

the limitation of the phase space

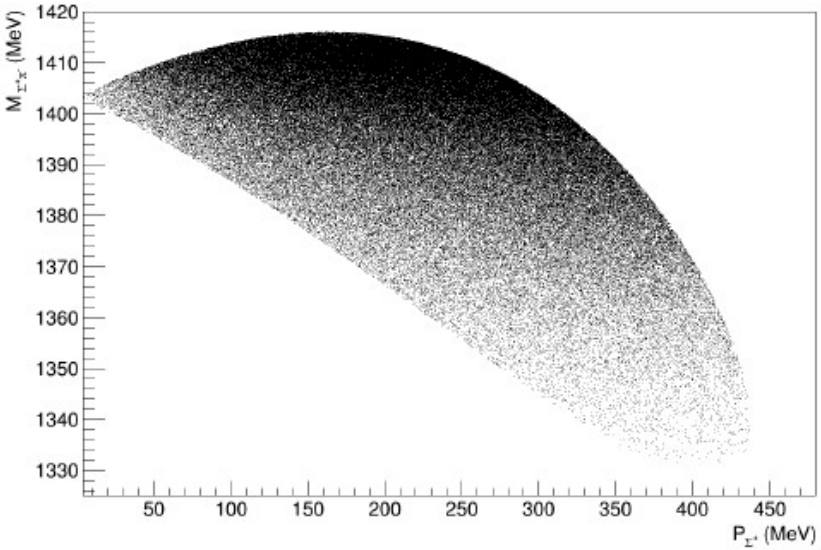

ThanK- you

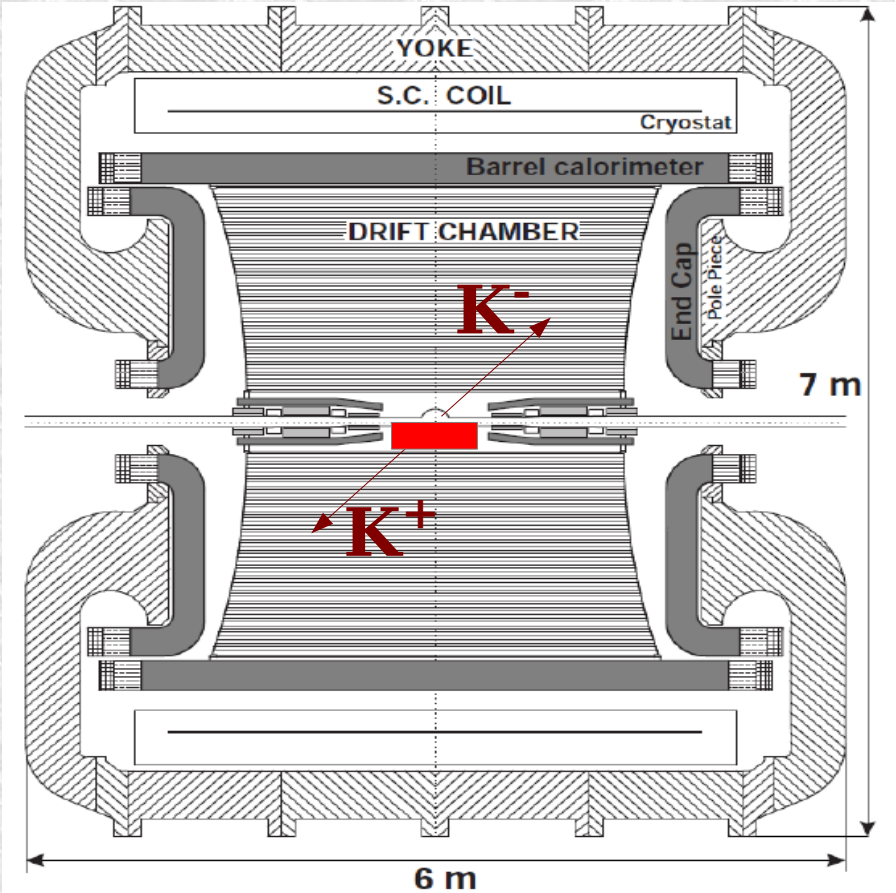
YOKE
S.C. COIL
Cryostat
Barrel calorimeter
DRIFT CHAMBER
End Cap
Pole Piece
K-
K+
7 m
6 m

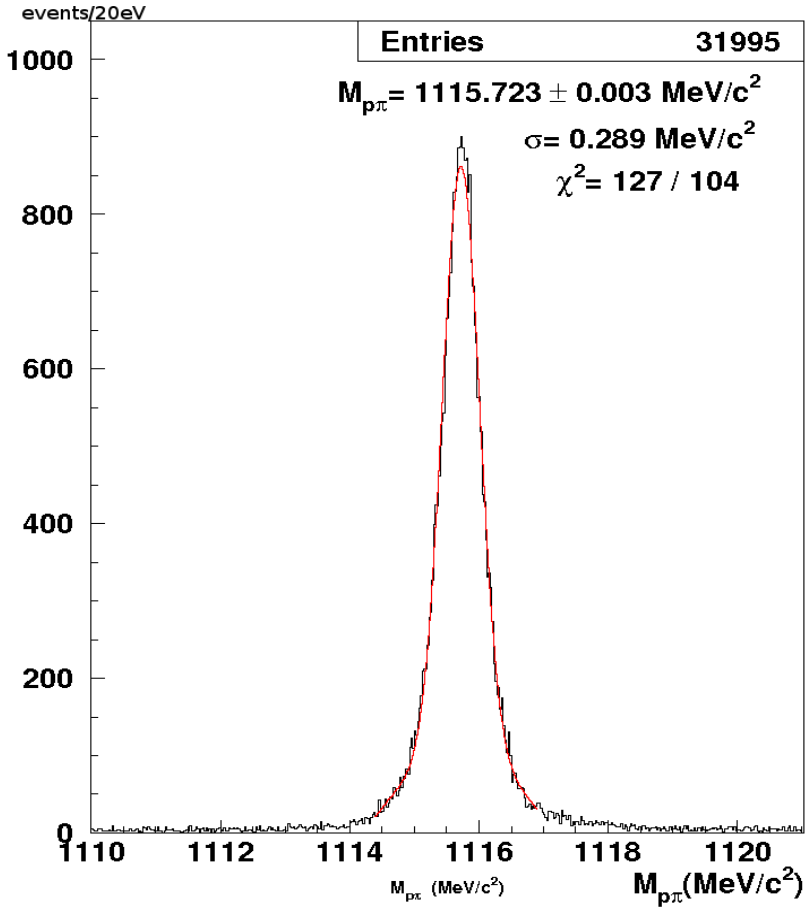
events/20eV
Entries 31995
$M_{p\pi}$= 1115.723 ± 0.003 MeV/c^2
σ= 0.289 MeV/c^2
χ^2= 127 / 104
$M_{p\pi}$ (MeV/c^2)
$M_{p\pi}$(MeV/c^2)

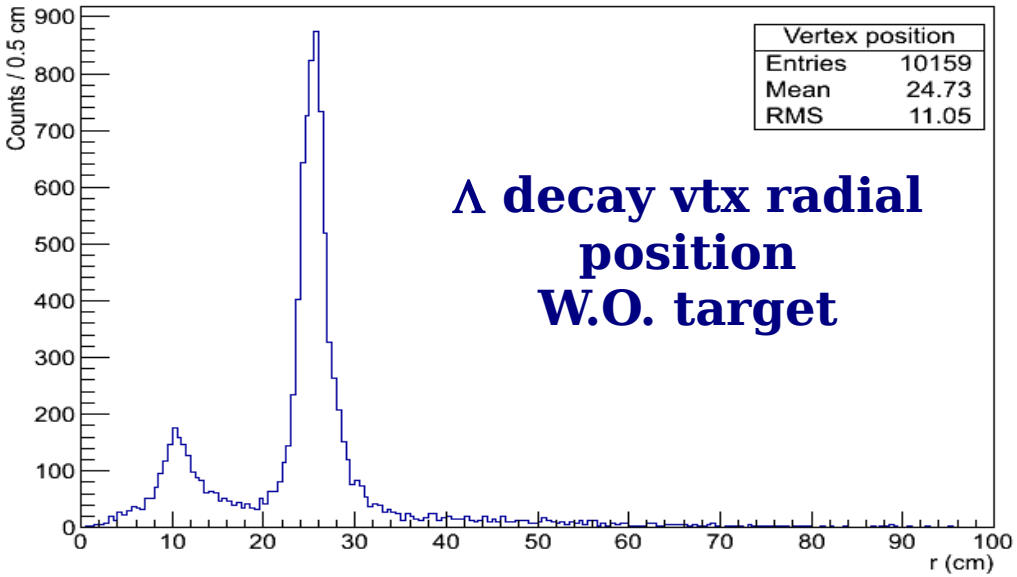
Counts / 0.5 cm
Vertex position
Entries 10159
Mean 24.73
RMS 11.05
Λ decay vtx radial position
W.O. target
r (cm)

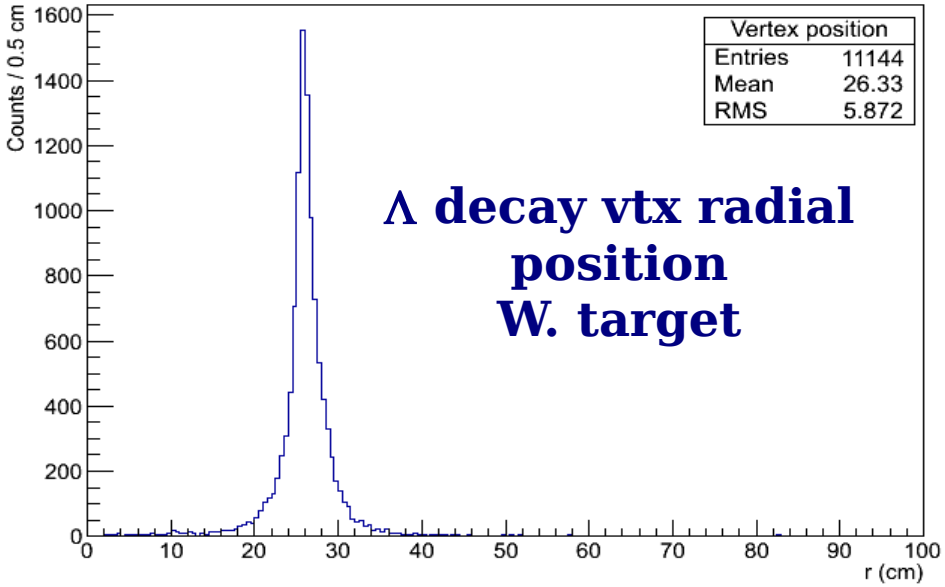
Counts / 0.5 cm
Vertex position
Entries 11144
Mean 26.33
RMS 5.872
Λ decay vtx radial position
W. target
r (cm)

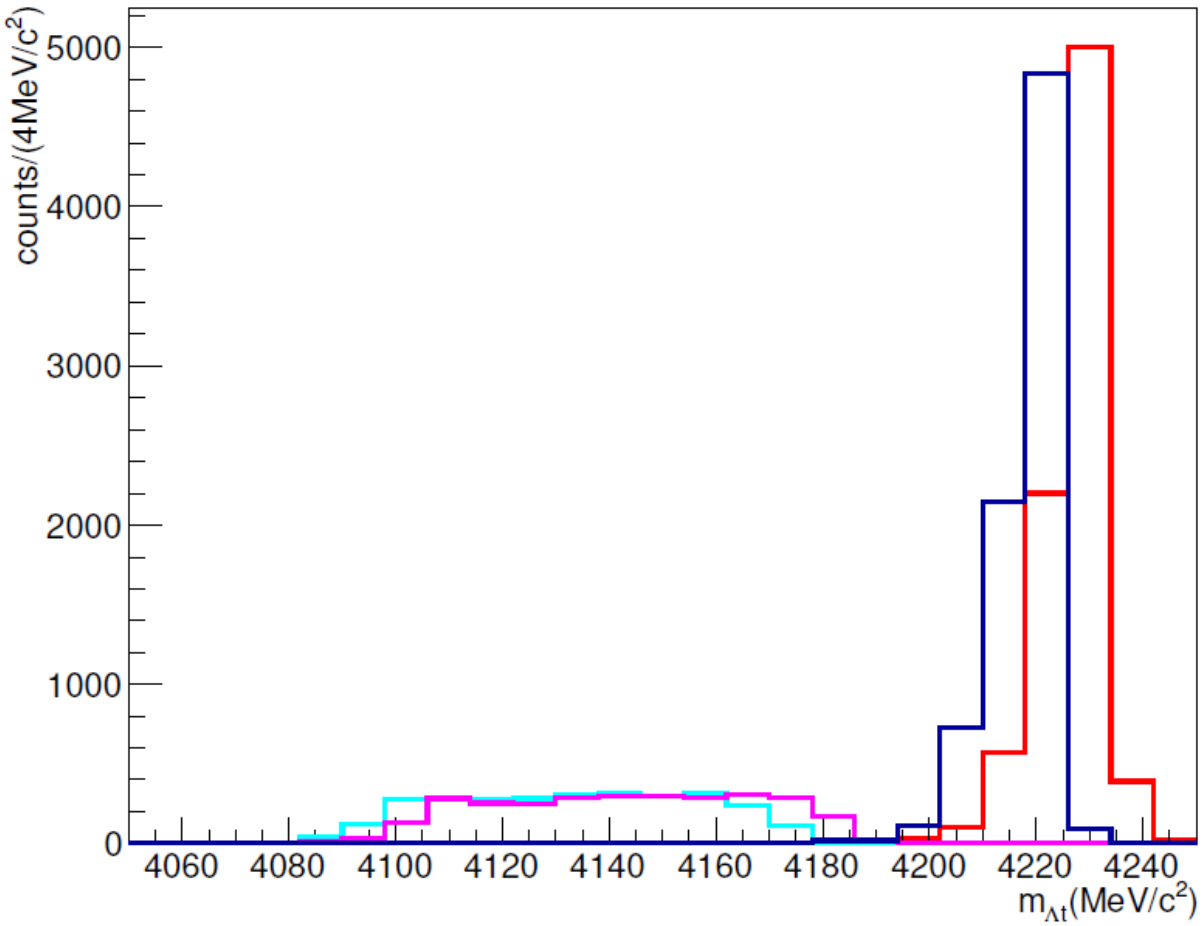

Figure 26. *Λ-t reconstructed invariant mass for the MC simulated processes: $K^{-4}He \rightarrow \Lambda t$ 4NA at-rest (blue), $K^{-4}He \rightarrow \Lambda t$ 4NA in-flight (red), $K^{-4}He \rightarrow \Sigma^0 t \rightarrow \Lambda\gamma t$ at-rest (cyan), $K^{-4}He \rightarrow \Sigma^0 t \rightarrow \Lambda\gamma t$ in-flight (magenta).*

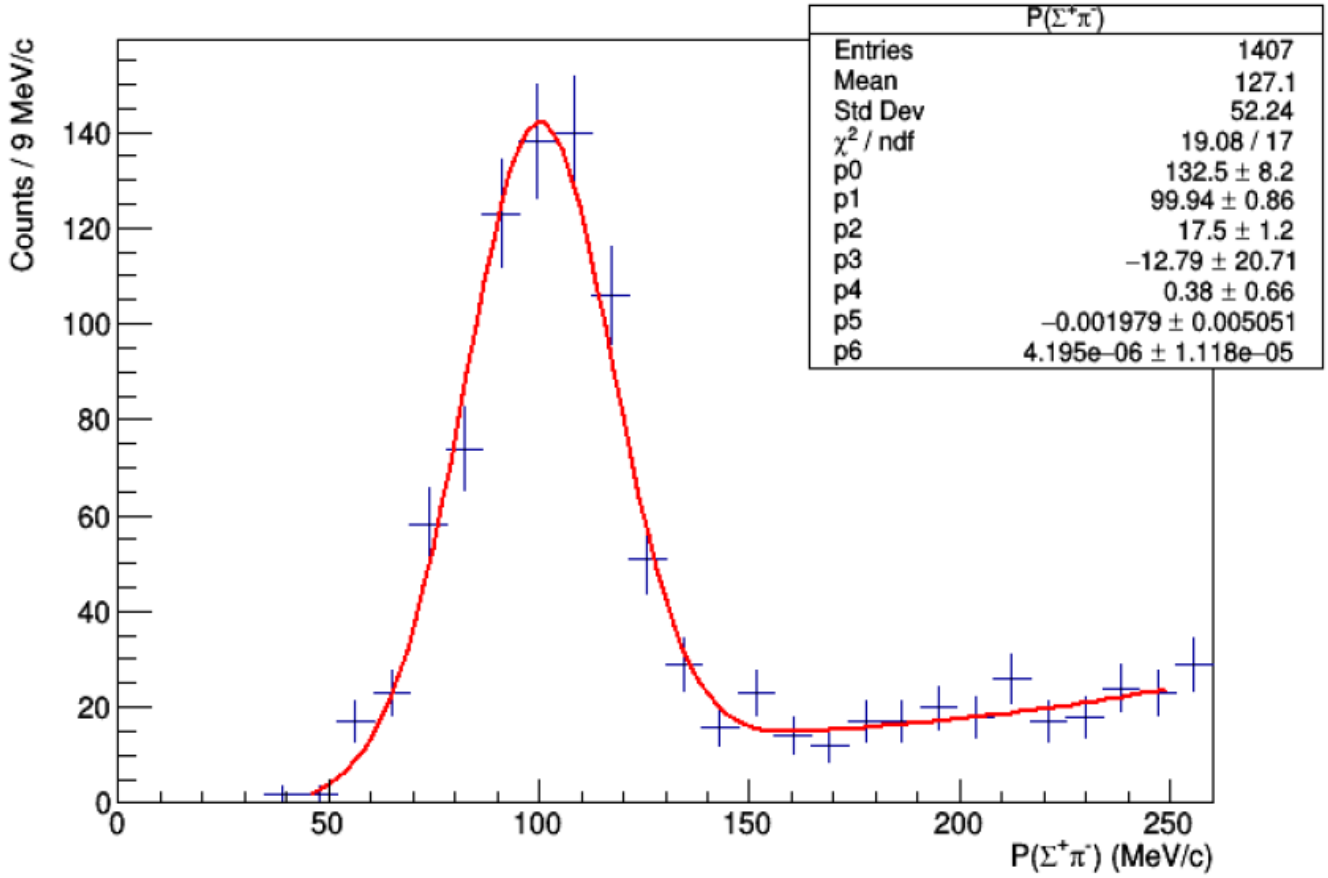

Figure 22. *Measured total $\Sigma^+\pi^-$ momentum distribution ($p_{\Sigma+\pi-}$) for the selected $K^-H \rightarrow \Sigma^+\pi^-$ events in-flight.*

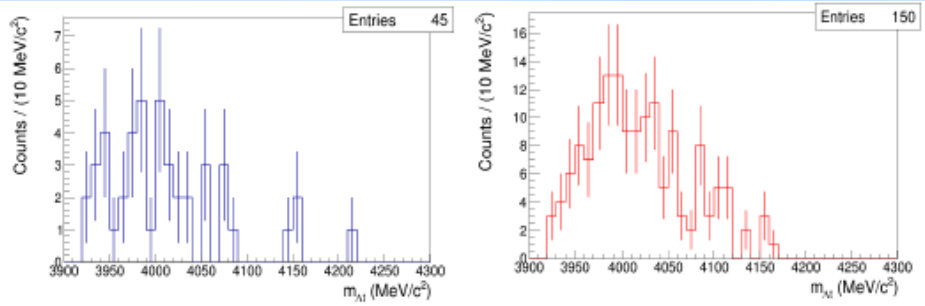

Figure 15. *Λt invariant mass distribution for $\Lambda t - p$ events generated in K^- gas absorptions (left), K^- wall absorptions (right)*

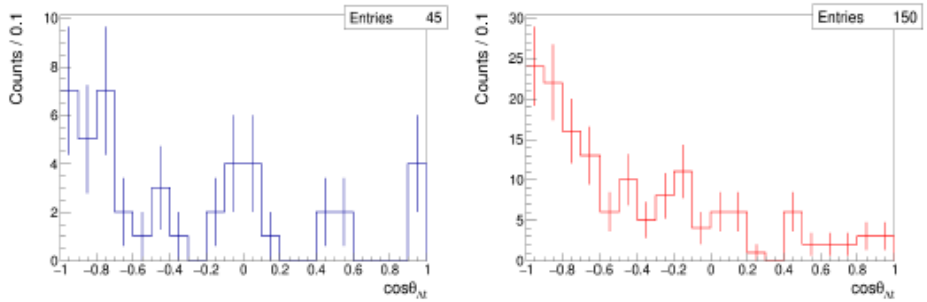

Figure 16. *$cos(\theta_{\Lambda t})$ distribution for $\Lambda t - p$ events generated in K^- gas absorptions (left), K^- wall absorptions (right)*

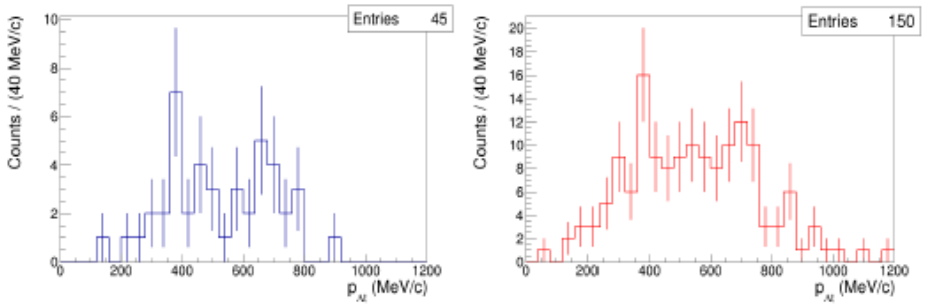

Figure 17. *$p_{\Lambda t}$ distribution for $\Lambda t - p$ events generated in K^- gas absorptions (left), K^- wall absorptions (right)*

The shapes of the three distributions for the two samples of $\Lambda t - p$ events are compatible, evidencing that the gas and the wall samples do not suffer, for the Λt channel, severe efficiency or acceptance differences. Moreover the ratios: ($\Lambda t - p$ events)/(total Λt events) for the gas and wall samples are 45/150 and 150/428 respectively, evidencing compatible detection efficiencies for the two samples.

Σ0 p correlated production, goals of this analysis

K- Absorption

- Pin down the contribution of the process:

$$K^- + NN \rightarrow \Sigma^0 + p$$

with respect to processes as:

$$K^- + NN \rightarrow \Sigma^0 + p \rightarrow p" + \Sigma^0" \; (FSI)$$

$$K^- + NNN \rightarrow \Sigma^0 + p + X$$

$$K^- + NNNN \rightarrow \Sigma^0 + p + X$$

Kaonic Bound States

$$ppK^- \rightarrow \Sigma^0 + p$$

- Yield Extraction and Significance

Absorption results

O. Vazquez Doce et al., Physics Letters B 758 (2016) 134

...is there room for the signal of a **ppK- bound state**?

Fit with ppK-

Best solution:

- **B.E. = 45 MeV/c2**
- **Width = 30 MeV/c2**

$$\chi^2 = 0.807$$

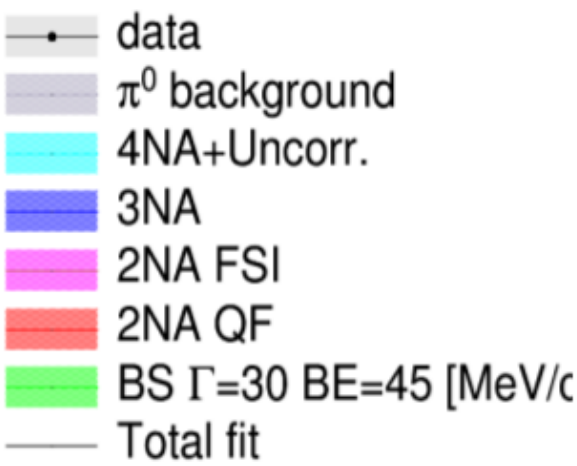

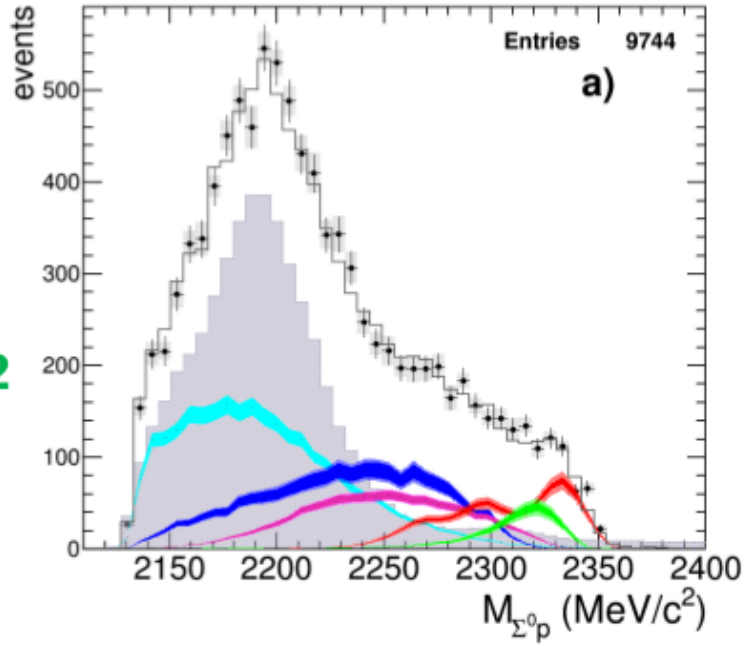

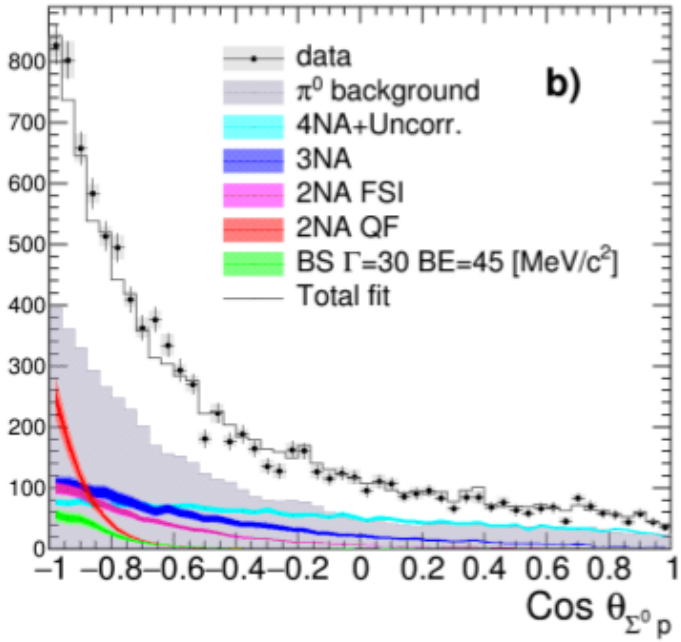

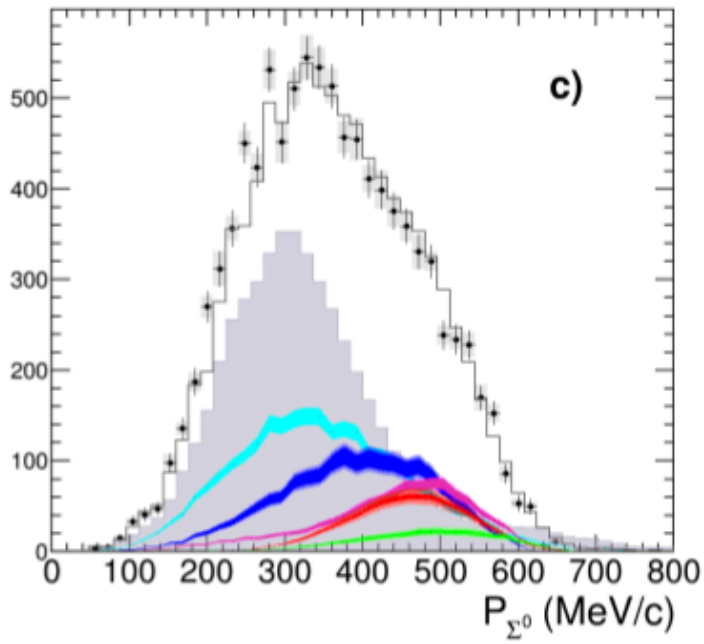

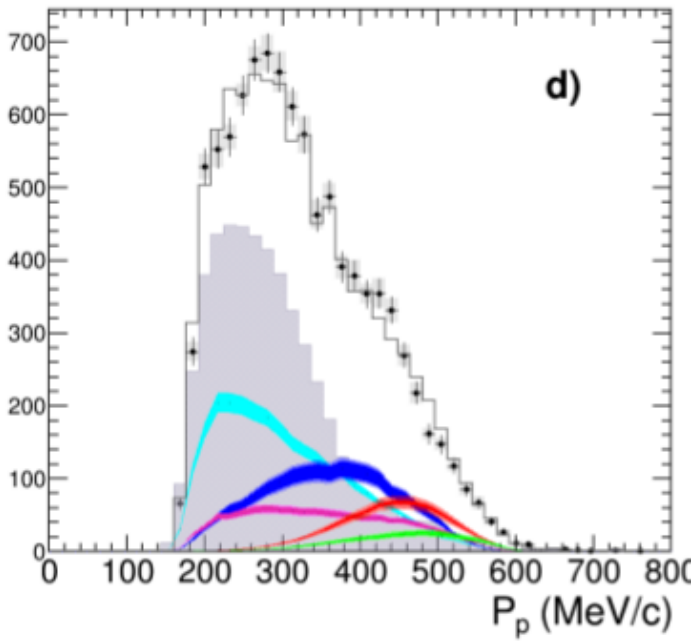

Evaluation of the significance of the ppK- signal

For B.E. = 45 MeV/c2, Width = 30 MeV/c2

$$Yield/K^-_{stop} = (0.044 \pm 0.009 stat^{+0.004}_{-0.005} syst) \cdot 10^{-2}$$

F-test to evaluate the addition of an extra parameter to the fit:

Significance of “signal” hypothesis w.r.t “Null-Hypothesis” (no bound state)

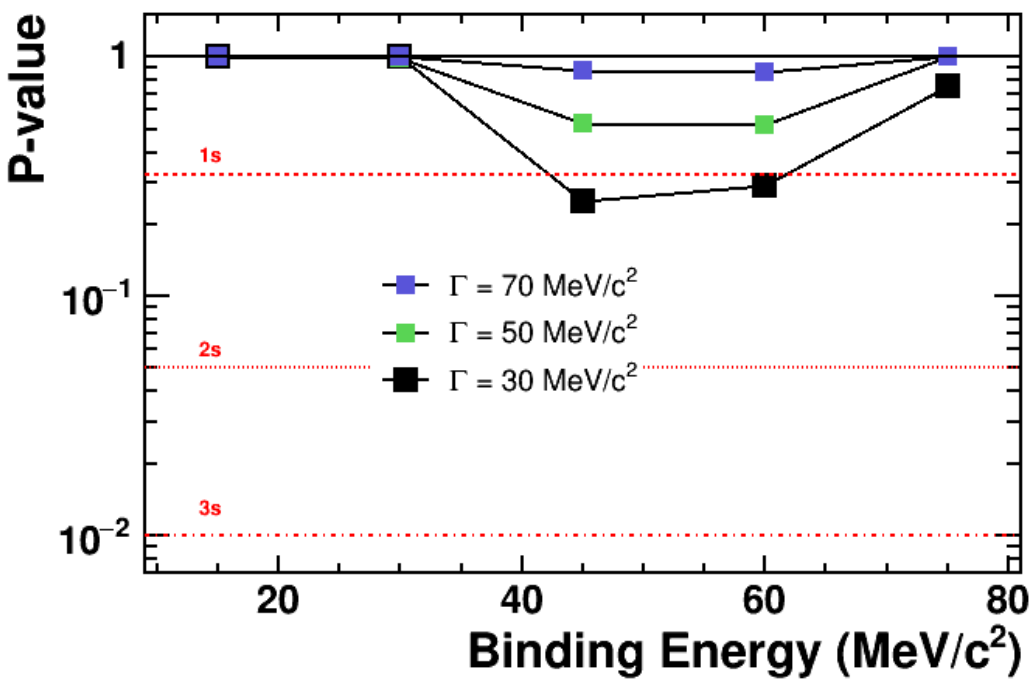

No significant detection of ppK- bound state